FLIGHT SIMULATION OF THE LONGITUDINAL MOTIONS OF ANOTHER AIRCRAFT

STEWART T. ZINK
and
RUSSELL E. WILTSIE

FLIGHT SIMULATION OF THE LONGITUDINAL MOTIONS OF ANOTHER AIRCRAFT

by

Lieutenant Stewart T. Zink, USN
Captain Russell E. Wiltsie, USMC

Aeronautical Engineering Report No. 508

May 1960

Submitted in partial fulfillment of the requirements for the Degree of Master of Science in Engineering from Princeton University, 1960

ACKNOWLEDGEMENT

The authors wish to acknowledge the very considerable assistance of many persons of the Department of Aeronautical Engineering, Princeton University, without whose help this project could not have been completed. These persons include: Professor E. Seckel, under whose supervision the studies were performed; Mr. E. J. Durbin, who very freely gave his time and unceasingly helped supervise the installation of the variable-stability system; Mr. Robert Cooper, airport manager, for his cooperation and expert help throughout the year; Mr. Ronald Meyer for his very expert and timely aid; Mr. William Bowen for his major part in the wiring installation; Mr. Richard Whitley for his trouble-shooting; Mr. Thomas Sweeney for his interest and assistance; Mr. Theodor Dukes for his interest and helpful suggestions; and the many others who had a part in the project.

Gratitude is also expressed to Mr. L. J. Devlin, Chief Engineer, Douglas Aircraft Company, Inc., and Mr. R. M. Chrone, Chief, Aero-Thermodynamics, North American Aviation, Inc., for their encouragement and service, to Lear, Inc., for auto-pilot parts and engineering drawings; and to Mr. Cornthwaite of the Naval Air Test Center, NAS Patuxent River, Maryland, for assistance in the location of test equipment.

TABLE OF CONTENTS

LIST OF SYMBOLS

C_{L_o}	Steady-state lift coefficient
C_{D_o}	Steady-state drag coefficient
C_{L_α}	Partial derivative of the lift coefficient with respect to angle of attack
C_{D_α}	Partial derivative of the drag coefficient with respect to angle of attack
C_{m_α}	Partial derivative of the moment coefficient with respect to angle of attack
$C_{m_{d\alpha}}$	Partial derivative of the moment coefficient with respect to $d\alpha = \tau\dot{\alpha}$
$C_{m_{d\theta}}$	Partial derivative of the moment coefficient with respect to $d\theta = \tau\dot{\theta}$
$C_{m_{\delta_e}}$	Partial derivative of the moment coefficient with respect to elevator deflection angle
C_{m_u}	Partial derivative of the moment coefficient with respect to non-dimensional velocity
α	Perturbation angle of attack, rad.
θ	Perturbation angle of pitch, rad.
u	Perturbation non-dimensional velocity
n	Perturbation normal acceleration
δ_e	Perturbation elevator angle, rad.
V	Velocity, ft./sec.
m	Mass of the aircraft, slugs
τ	$(\equiv \frac{m}{\rho SV})$, sec.

LIST OF SYMBOLS

I_Y	Moment of inertia about Y-axis, slug ft.^{2}
h	$\left[\equiv \frac{2}{\mu}\left(\frac{K_y}{\bar{c}}\right)^2\right]$
μ	$\left[\equiv \frac{m}{\rho S\bar{c}}\right]$, density factor
K_y	$\left[\equiv \sqrt{\frac{I_Y}{m}}\right]$, radius of gyration, ft.
$\bar{c}$	Mean aerodynamic chord, ft.
S	Wing area, ft.^{2}
A	Aspect ratio
b	Wing span, ft.
$\triangle$	Denominator term of a transfer function
N	Numerator term of a transfer function
(s)	LaPlacian transform symbol
K	Gain
ζ	Damping ratio
ω_n	Natural frequency

Subscripts:

s.s.	Steady-state
phu.	Phugoid mode
s.p.	Short period mode

FLIGHT SIMULATION OF THE LONGITUDINAL MOTIONS OF ANOTHER AIRCRAFT

SUMMARY

Simulation of the control-fixed longitudinal dynamic characteristics of the A4D-2, a Douglas jet attack aircraft, was attempted with use of a variable-stability airplane, Princeton University's North American Navion, and with telemetry for data presentation. The variable-stability installation was built as a joint project for both longitudinal and lateral-directional studies, and although the attempt at simulation of the A4D-2 was not successful, it is hoped that suitable guide lines have been established for similar studies. As a secondary objective, the effects of feeding back the airplane responses u, α, $\dot{\theta}$ and θ were investigated.

The project commenced in October 1959 at Forrestal Research Center, Princeton University, Princeton, New Jersey, and was completed in May 1960.

FLIGHT SIMULATION OF THE LONGITUDINAL MOTIONS OF ANOTHER AIRCRAFT

INTRODUCTION

Variable-stability aircraft and their use in flight research have received increased emphasis with the advent of sonic and supersonic aircraft. To date, much work has been done along these lines, primarily by Cornell Aeronautical Laboratory, Inc., and the NACA (now NASA). For longitudinal studies in particular, several aircraft including a C-45, an F-94, a B-26, and a T-33, have been variously configured by Cornell Aeronautical Laboratory with electro-hydraulic systems used to modify elevator and other auxiliary control surface responses, in order that studies could be made of:

1) aircraft natural modes that are essentially aperiodic and convergent;
2) optimum handling characteristics;
3) proposed handling characteristics of an aircraft in design stages;
4) inertia effects;
5) phugoid damping.

Similarly, the NACA has devoted much effort towards such studies, also by use of variously configured variable-stability aircraft. Refs. 1 through 8 apply.

In this report, simulation of the longitudinal response characteristics of the A4D-2, the Douglas attack jet aircraft, was attempted with a North American Navion configured as a variable-stability aircraft. Only specific response characteristics of the phugoid and short period were studied, not pilot opinion or handling qualities, since stick-force gradients and the like were not provided.

The variable-stability installation built in Princeton University's North American Navion was constructed around a 3-axes, stick-steering, attitude-and-rate-sensing auto-pilot. Electrical signals produced by various transducers were summed in the auto-pilot summing circuits, and the control surfaces were moved by electrical servos through the ship's control cable system in proportion to these signals. The variable-stability installation was used to alter the normal stability derivatives of the Navion and to introduce additional or psuedo-stability derivatives, thereby changing the aircraft dynamic response characteristics.

The auto-pilot installation was a joint project in which both longitudinal and lateral-directional characteristics were studied. The other half of the joint project, lateral-directional, is described in Ref. 9. All studies were performed at the Forrestal Research Center, Princeton University, during the academic year 1959-1960.

THEORY AND ANALYSIS

The normal procedure in the determination of aircraft dynamic motions is to solve the simultaneous, constant-coefficient, linear differential equations of motion that characterize the transient response of the aircraft to a disturbance from some equilibrium flight condition. This procedure is outlined in Ref. 10. In the determination of the design requirements of the variable-stability installation, the longitudinal equations of motion of both the Navion and the A4D-2 were compared as outlined below.

EQUATIONS OF MOTION

The longitudinal (stick-fixed) equations of motion may be written as follows, in non-dimensional time with the angles in radians:

$$(C_{D_{eff}} + d)u + 1/2(C_{D_\alpha} - C_L)\alpha + \frac{C_L}{2}\theta = 0 \qquad (1)$$

$$C_{L_{eff}}u + (\frac{C_{L_\alpha}}{2} + d)\alpha - d\theta = 0 \qquad (2)$$

$$C_{m_u}u + (C_{m_\alpha} + C_{m_{d\alpha}}d)\alpha + (C_{m_{d\theta}}d - hd^2)\theta = -C_{m_{\delta_e}}\delta_e \qquad (3)$$

where: $C_{D_{eff}} \equiv C_{D_o} + \frac{M}{2}\cdot\frac{\partial C_D}{\partial M} - \frac{1}{\rho SV}\cdot\frac{\partial T}{\partial V}$

$C_{L_{eff}} \equiv C_{L_o} + \frac{M}{2}\cdot\frac{\partial C_L}{\partial M} + 1/2\,\frac{\partial C_L}{\partial u}$

$d(\;) \equiv \frac{d(\;)}{d(t/\tau)}$

$h \equiv \frac{2}{\mu}\left(\frac{K_y}{\bar{c}}\right)^2$, inertia factor

$\mu \equiv \frac{m}{\rho S\bar{c}}$, density factor

Now let the forcing function, δ_e, take the following non-dimensional form with angles in radians;

$$\delta_e = K_s \delta_s + K_1 \alpha + \frac{K_2}{\tau} d\theta + K_3 u + K_4 \theta \qquad (4)$$

where K_1, K_2, K_3, and K_4 hereafter will be referred to as gain constants. Equation (4) may also be written as:

$$\delta_e = \left(\frac{\Delta\delta e}{\Delta\delta_s}\right)\delta_s + \left(\frac{\Delta\delta e}{\Delta\alpha}\right)\alpha + \left(\frac{\Delta\delta e}{\Delta\dot{\theta}}\right)\dot{\theta} + \left(\frac{\Delta\delta e}{\Delta u}\right)u$$

$$+ \left(\frac{\Delta\delta e}{\Delta\theta}\right)\theta, \qquad (5)$$

where δ_s, u, α, $\dot{\theta}$ and θ are understood to be perturbation quantities.

Substituting δ_e into the moment equation:

$$(C_{m_u})u + (C_{m_\alpha} + C_{m_{d\alpha}} d)\alpha + (C_{m_{d\theta}} d - hd^2)\theta = -C_{m_{\delta_e}} K_s \delta_s$$

$$- C_{m_{\delta_e}} K_1 \alpha - C_{m_{\delta_e}} \frac{K_2}{\tau} d\theta - C_{m_{\delta_e}} K_3 u - C_{m_{\delta_e}} K_4 \theta$$

To write the moment equation in real time, $p = \frac{1}{\tau} d$. Transposing and collecting terms:

$$(C_{m_u} + C_{m_{\delta_e}} K_3)u + (C_{m_\alpha} + C_{m_{d\alpha}} \tau p + C_{m_{\delta_e}} K_1)\alpha + (C_{m_{\delta_e}} K_4$$

$$+ C_{m_{d\theta}} \tau p - h\tau^2 p^2 + C_{m_{\delta_e}} K_2 p)\theta = -C_{m_{\delta_e}} K_s \delta_s$$

$$\text{or } C_{m_u} G_3 u + (C_{m_\alpha} G_1 + C_{m_{d\alpha}} \tau p)\alpha + (C_{m_{\delta_e}} K_4 + C_{m_{d\theta}} G_2 \tau p$$

$$- h\tau^2 p^2)\theta = -C_{m_{\delta_e}} K_s \delta_s \qquad (6)$$

where: $$G_1 = 1 + \frac{C_{m_{\delta_e}}}{C_{m_\alpha}} K_1$$

$$G_2 = 1 + \frac{C_{m_{\delta_e}}}{C_{m_{d\theta}}} \frac{K_2}{\tau}$$

$$G_3 = 1 + \frac{C_{m_{\delta_e}}}{C_{m_u}} K_3$$

Expressing all the equations in a determinent form in real time:

$$\begin{array}{llll}
u & \alpha & \theta & \delta \\
C_{D_{eff}} + \tau p & 1/2(C_{D_\alpha} - C_L) & C_L/2 & 0 \\
C_{L_{eff}} & \frac{C_{L_\alpha}}{2} + \tau p & -\tau p & 0 \\
C_{m_u} G_3 & C_{m_\alpha} G_1 + C_{m_{d\alpha}} \tau p & C_{m_{\delta_e}} K_4 + C_{m_{d\theta}} G_2 \tau p & -C_{m_{\delta_e}} K_s \delta_s \\
 & & - h \tau^2 p^2 &
\end{array}$$

GAIN CONSTANTS

Solutions to these equations of motion were obtained by assuming the solution of the form:

$$u = u_1 e^{\lambda t/\tau} \qquad \alpha = \alpha_1 e^{\lambda t/\tau} \qquad \theta = \theta_1 e^{\lambda t/\tau}$$

Upon substitution of these variables into the equations of motion, together with their first and second derivatives, three homogeneous algebraic equations resulted. Further, expansion of the resultant determinant gave the standard quartic equation in λ, implicitly in terms of the gain constants, as shown:

$$c_4\lambda^4 + c_3\lambda^3 + c_2\lambda^2 + c_1\lambda + c_o = 0 \tag{7}$$

where:

$$C_4 = -h\tau^4 \tag{8}$$

$$C_3 = \tau^3\left[C_{m_{d\theta}}G2 + C_{m_{d\alpha}} - h\left(\frac{C_{L_\alpha}}{2} + C_{D_{eff}}\right)\right] \tag{9}$$

$$\begin{aligned} C_2 = \tau^2\Big[& C_{D_{eff}}\left(C_{m_{d\alpha}} + C_{m_{d\theta}}G2 - \frac{C_{L_\alpha}}{2}h\right) + \frac{hC_{L_{eff}}}{2}\left(C_{D_\alpha} - C_L\right) \\ & + \frac{C_{L_\alpha}}{2}C_{m_{d\theta}}G2 + C_{m_\alpha}G1 + K_4C_{m_{\delta_e}}\Big] \end{aligned} \tag{10}$$

$$\begin{aligned} C_1 = \tau\Big[& C_{D_{eff}}\left(\frac{C_{L_\alpha}}{2}C_{m_{d\theta}}G2 + C_{m_\alpha}G1\right) + \frac{C_LC_{L_{eff}}}{2}\Big(C_{m_{d\theta}}G2 \\ & + C_{m_{d\alpha}} - \frac{C_{D_\alpha}}{C_L}C_{m_{d\theta}}G2\Big) - \frac{C_{m_u}}{2}G_3C_{D_\alpha} \\ & + K_4C_{m\delta_e}\left(C_{D_{eff}} + \frac{C_{L_\alpha}}{2}\right)\Big] \end{aligned} \tag{11}$$

$$\begin{aligned} C_o = \frac{C_L}{2}\left[C_{L_{eff}}C_{m_\alpha}G_1 - C_{m_u}\frac{C_{L_\alpha}}{2}G_3\right] + K_4\frac{C_{m\delta_e}}{2}\Big[& C_{D_{eff}}C_{L_\alpha} \\ & - C_{L_{eff}}\left(C_{D_\alpha} - C_L\right)\Big] \end{aligned} \tag{12}$$

In terms of modified transfer functions, the numerator terms were found to be:

$$N_\alpha = -C_{m\delta_e}K_s\delta_s\left[\tau^2p^2 + \tau pC_{D_{eff}} + \frac{C_L}{2}C_{L_{eff}}\right] \tag{13}$$

$$N_u = +\frac{C_{m\delta_e}}{2}K_s\delta_s\left[C_{D_\alpha}\tau p + C_{L_\alpha}\frac{C_L}{2}\right] \tag{14}$$

$$\begin{aligned} N_\theta = -C_{m\delta_e}K_s\delta_s\Big[& \tau^2p^2 + \tau p\left(\frac{C_{L_\alpha}}{2} + C_{d_{eff}}\right) \\ & + C_{D_{eff}}\frac{C_{L_\alpha}}{2} - C_{L_{eff}}\frac{C_{D_\alpha}}{2} + C_{L_{eff}}\frac{C_L}{2}\Big] \end{aligned} \tag{15}$$

Evaluation of the coefficients of the characteristic equation, in terms of the Navion stability derivatives as shown in Appendix A, yielded the following relations explicit in the gain constants:

$$C_4 = 1 \tag{16}$$

$$C_3 = 5.30 + 15.75\ K_2 \tag{17}$$

$$C_2 = 9.88 + 15.74\ K_1 + 32.27\ K_2 + 15.73\ K_4 \tag{18}$$

$$C_1 = .408 + .468\ K_1 + 1.284\ K_2 - 1.942\ K_3 + 32.25\ K_4 \tag{19}$$

$$C_o = .355 + 1.051\ K_1 - 5.81\ K_3 + 1.285\ K_4 \tag{20}$$

Also as shown in Appendix A, like constants of the characteristic equations of the Navion and the A4D-2 were equated in the following fashion, and solutions for the gain constants were found:

$$(C_4^{\dagger})_{A4D-2} = (C_4)_{MOD.\ NAV.}$$

$$(C_3^{\dagger})_{A4D-2} = (C_3)_{MOD.NAV.}$$

and so on, where the notation "Mod. Nav." refers to Modified Navion. The gain constants were found to be as follows:

$K_1 = -\ .0407 \qquad \left(= \frac{\Delta \delta e}{\Delta \alpha}\right)$

$K_2 = -\ .240 \qquad \left(= \frac{\Delta \delta e}{\Delta \dot{\theta}}\right)$

$K_3 = .0465 \qquad \left(= \frac{\Delta \delta e}{\Delta u}\right)$

$K_4 = .0033 \qquad \left(= \frac{\Delta \delta e}{\Delta \theta}\right)$

SIGNIFICANCE OF GAIN CONSTANTS

As may be seen in Equation (6), additional airplane moments were added to the longitudinal moment equation. For instance, the $C_{m_u} G_3 u$ term is implicitly composed of the two terms $C_{m_u} + C_{m_{\delta_e}} K_3$, where $C_{m_{\delta_e}} K_3$ is a moment increment added to the original moment C_{m_u}. Then the individual moments are as follows:

$$C_{m_u} + C_{m_{\delta_e}} K_3 = C_{m_u} + \Delta C_{m_u} \qquad (21)$$

$$C_{m_\alpha} + C_{m_{\delta_e}} K_1 = C_{m_\alpha} + \Delta C_{m_\alpha} \qquad (22)$$

$$C_{m_\theta} + C_{m_{\delta_e}} K_4 = C_{m_\theta} + \Delta C_{m_\theta} \qquad (23)$$

$$C_{m_{d\theta}} + C_{m_{\delta_e}} \frac{K_2}{\tau} = C_{m_{d\theta}} + \Delta C_{m_{d\theta}} \qquad (24)$$

Examination of these equations shows the following:

1) for the Navion, $C_{m_u} = 0$, so ΔC_{m_u} amounts to a pseudo static stability derivative;

2) the same applies to ΔC_{m_θ};

3) since aircraft responses to α and $\dot{\theta}$ already exist, ΔC_{m_α} and $\Delta C_{m_{d\theta}}$ amount to altered stability derivatives and changed response characteristics of the aircraft.

Signs of the gain constants indicate that K_1 through K_3 supply destabilizing moments, while K_4 supplies a stabilizing moment. A study of the magnitudes of the gain constants shows the following:

1) K_1: for a positive 15° increase in angle of attack, the variable-stability installation must apply $.6^\circ$ of up elevator;

2) K_2: for a positive pitch rate of 5°/sec., 1.2° up elevator;

3) K_3: for an increase in speed of 12 mph, .3° down elevator; and

4) K_4: for a positive 15° increase in pitch angle, .05° down elevator.

As was shown by Equations (13) through (15), the forcing function $C_{m_{\delta_e}} K_s \delta_s$ (which is effectively $C_{m_{\delta_e}} \delta_e$) appears in the numerators, but the gain constants do not so appear. This is clearly the result of making changes only to the moment equation, and none to the lift and drag equations. The above indicated that with provisions only for modifying moments, no simulation could be made of:

1) amplitude of oscillations in u, α, θ, and $\dot{\theta}$ during transient responses, and

2) steady-state values of the above for say an elevator step input forcing function.

It was seen, however, that this would not limit simulation of the transient response characteristics damping and frequency.

PROCEDURE AND EQUIPMENT

ANALYTICAL STUDIES

It was decided that a complete analytical study should precede the flight simulation, with particular emphasis on the magnitude of acceleration normal to the aircraft's flight path, and some emphasis on the effects of the impossibility of simulating aircraft transfer functions of the A4D-2. In order to accomplish the above, a computer program utilizing the Goodyear Geda Analog Computer was organized. The dynamic response characteristics of the A4D-2 were studied first, and damping and frequency of each of the two longitudinal response modes, short period and phugoid, were determined from the computer and compared with those obtained by analytical methods.

For comparison, response characteristics of the unmodified Navion were also determined, as outlined in Appendix B. Then by use of the computer the simulation of the A4D-2 was accomplished, and the effects of variations of gain constants were studied. Normal accelerations, primarily during the short period, were calculated, also as outlined in Appendix B.

In addition to the above, studies were made of the effects of the gain constants on aircraft response as each individual gain constant was fed back with increasing magnitude from a zero value.

DESIGN OF THE AUTO-PILOT

Simultaneously with the initial theoretical studies of the variable-stability installation, physical design considerations of the auto-pilot variable-stability combination were examined. The first step was a flight test program to determine control cable forces encountered in the Navion during maneuvering flight. Flight test instrumentation used in these

flight tests was kept simple to avoid an excessive delay in the construction of the auto-pilot. Test instruments included a hand-held spring force gage, a glass tube-and-spring accelerometer, and elevator, aileron, and rudder control position indicators, which consisted of markings on bulkheads of the aircraft close to the respective control and pointers attached to the cockpit controls. Since auto-pilot construction had already begun on Navion N91566, Princeton University's second Navion, N5113K, which is essentially an identical airplane, was used for the flight tests.

Flight tests consisted of one flight where measurements were taken of control stick force per g, stick force per velocity, and rudder and aileron control force per deflection of each. Control stick force per g was measured in steady turns, stick force per velocity was measured over a range of velocity below and above the trim speed, 122 m.p.h., in 10 m.p.h. increments, and rudder and aileron control force per deflection were measured in steady sideslips. One test altitude was used, 3000 ft., and one configuration: landing gear and flaps up, canopy closed, cowl flaps closed, mixture rich, 1900 rpm, and 22 in. of manifold pressure. All tests were performed as outlined in Refs. 13 and 14.

With the Navion on the ground, the hand-held spring force gage was used to determine control cable forces encountered during the above flight test work. Although measurements of control cable forces were made difficult by a cross-control coupling between the aileron and rudder cables, it was believed that these forces could be subtracted out with sufficient accuracy for design purposes. It was subsequently accomplished in this manner.

Cable force determination was the linking step to the determination of required servo pulley gearing ratios. The two basic considerations involved in the gearing ratios were whether the given servo-pulley combination, with 160 in. lb. design torque, could provide the required cable forces, and whether the speed of response of the servos was such that the airplane-auto-pilot combination would be dynamically stable. The latter consideration is outlined in detail in Ref. 9, and the result of both considerations led to the design and construction of a larger servo pulley for the longitudinal axis for better speed of response. Existing lateral and directional servo pulleys were found to be satisfactory.

With the help of detailed blueprints and some parts of a Lear, Inc. electric auto-pilot specifically designed for the Navion, location of separate variable-stability auto-pilot components was decided. With limited space available in the Navion, and with the existing arrangement of control cables, the logical location of the three-axis servo installation was the center of the bulkhead at the after end of the baggage compartment. Design and construction of the servo support mountings and brackets commenced early in November. Design and construction of the electrical and electronic components got underway about the same time, as outlined in Ref. 9.

Angle of attack and sideslip angle sensors were procured from the Naval Air Test Center, Patuxent River. By use of a probe, previously designed for similar measurements, the angle of attack and sideslip angle sensors were mounted in tandem, approximately one and one-half chord lengths ahead of the leading edge of the left wing, at the tip. The dynamic and static pressure probe, also previously designed, was mounted on the right wing-tip,

also approximately one and one-half chord lengths ahead of the leading edge; the transducer used for pressure (airspeed) measurements was located just inside the right wing tip bow.

An electrical stick and rudder was designed and installed as described in Ref. 9, along with the feed-back gain potentiometers and their mountings. The balance of electrical and electronic equipment including telemetry was designed and was installed in the baggage compartment; see Ref. 9.

When the servo and pulley installation had been completed, elevator servo cables were fed aft from the servo installation and tied into the ship's elevator cables at a small angle, with use of cable tie-ins provided by Lear; aileron servo cables were fed forward through a pulley system to the then existing aileron follow-up cables, and rudder servo cables were fed aft through a single pulley to the ship's rudder cables. Tension on the ship's cables was set at 30 lbs., as per Navion maintenance specifications, and tension in servo cables was set at 25 lbs.

Servo clutch slip levels were set such that the safety pilot, with use of the ship's controls, could, for example, over-ride the elevator servo of the auto-pilot with 16 lbs. of control force. In terms of torque limits for over-ride, slip levels were set as follows: elevator servo, 160 in. lbs.; aileron servo, 100 in. lbs.; rudder servo, 60 in. lbs. These levels were designed to permit control of the airplane in the cases of either inadvertent engaging of the auto-pilot, or failure of the auto-pilot disengaging system.

Electrical and mechanical installations were mostly completed by the middle of February, and a complete static (ground) test of the servo system was inaugurated. The static check included:

1) setting the servo limit switches;
2) with full control deflection, checking the slack sides of the control cables for tension;
3) measuring the control force required to overpower the auto-pilot;
4) observing the structural effects on the servo and pulley installation, and surrounding mountings, during maximum force tests;
5) observing all cables for excessive cable stretch during rapid, large deflections of all controls;
6) checking the complete aircraft control system for proper and safe operation;
7) inspecting the aircraft structurally after completion of the above; and
8) testing for total weight and aircraft center of gravity location.

Upon completion of the static tests and electrical trouble-shooting, at the end of March, the aircraft was test-flown to determine possible discrepancies of the aircraft and the auto-pilot installation. After the test flights, the Navion was given a somewhat less strenuous but thorough static check.

CALIBRATIONS

Calibrations consisted essentially of determining first the number of degrees of control surface deflection per volt input to the servo, for a given servo feed-back gain, and second the magnitude of input signal from

each transducer for particular potentiometer settings, e.g., the number of volts input from the angle of attack vane at 5° angle of attack, with a potentiometer setting of 0.1. The four sensors of the longitudinal channel, angle of attack vane, pressure (airspeed) transducer, pitch gyro and pitch-rate gyro, were calibrated in this fashion, as was the electrical stick. Aircraft response quantities which were to be telemetered, the four above plus elevator servo position (elevator position) were calibrated also; this amounted to measuring the telemeter d.c. output voltage for an a.c. transducer signal input.

FLIGHT TEST PROGRAM

The flight test program consisted of three flights which were necessary to trouble-shoot communications, telemetry, and auto-pilot electronics, and one flight during which test data was taken. Time did not permit further testing.

The configuration tested was as follows: landing gear and flaps up, canopy closed, oil cooler doors open, 1850 r.p.m., and approximately 20 in. of manifold pressure. Test altitude was 6500 ft., and airspeed was 110 m.p.h. indicated (120 m.p.h. true). The forcing functions utilized in the tests consisted of approximately .05 rad. elevator steps or impulses; these were provided by the auto-pilot with deflection of the electric stick, which had been calibrated to produce approximately .05 rad. of elevator deflection for full aft deflection of the stick. Also, during phugoid tests, the wings were held level by use of the auto-pilot rudder controls.

First, dynamic characteristics of the basic Navion were tested with the auto-pilot and the elevator step forcing function; with telemetry, the dynamic response characteristics were recorded on magnetic tape by an

Ampex 309-C tape recorder and on time history traces by a Sanborn 150 recorder. Second, with an arbitrary gain potentiometer setting of .15 for the u feed-back, and with the auto-pilot and a .05 rad. impulse forcing function, the short period and phugoid motions of the modified Navion were tested and recorded. In similar fashion, the α , $\dot{\theta}$, and θ feed-backs were tested. After the completion of each test run, the auto-pilot was disengaged, the aircraft was flown back to test altitude and test airspeed, and the auto-pilot was re-engaged.

For reasons outlined in later sections, the simulation of the A4D-2 was not attempted.

RESULTS AND DISCUSSION

GENERAL RESULTS

The primary objective, that of in-flight simulation of the A4D-2 with the Navion and its variable-stability installation, was not accomplished because of the effects outlined below. The secondary objective, which developed during the theoretical analysis of the simulation, that of an investigation of the effects of variation of the feed-back quantities on airplane dynamic response, was accomplished through a theoretical analysis, but was not verified by flight test data. However, it is felt that the information contained herein concerning the variable-stability installation and the attempted simulation should be of help in establishing guide lines for similar studies.

ANALYTICAL RESULTS

As outlined in some detail in Appendix B, a comparison of the dynamic characteristics of the two aircraft, the A4D-2 and the Navion, was made. For ease of comparison, these characteristics are repeated here; factorization of the two characteristic equations gave, in seconds:

Airplane	Phugoid		Short Period	
	P	$T_{1/2}$	P	$T_{1/2}$
A4D-2	34.9	39.5	6.59	.94
Navion	32.9	62.6	3.78	.26

From the above, it may be seen that the variable-stability installation had to be designed to change the dynamic characteristics of the Navion in the following way: decrease the frequency of the phugoid and the short period modes, decrease the damping of the short period mode, and increase the damping of the phugoid mode. As outlined in the section on theoretical considerations, such changes were provided for by the use of the feed-backs $u, \alpha, \dot{\theta}$, and θ, and the related gain constants were found to be of particular magnitudes and algebraic signs.

At this point it should be re-emphasized that the characteristic equation of the Navion was made exactly similar to that of the A4D-2 by use of the feed-backs, but, in terms of transfer functions, the numerator terms were in no way changed. The transfer functions of the modified Navion then consisted of a constant comprised of Navion stability derivatives, a fourth order denominator term peculiar to the A4D-2, and a first or second order numerator term peculiar to the Navion.

As outlined in Appendix B, the effects of this kind of matching were investigated. In a comparison of steady-state values, i.e., the magnitudes of the perturbation quantities $u, \alpha, \dot{\theta}$, and θ as $t \to \infty$, the same amount of elevator deflection used as a step forcing function produced markedly different results. For example, a .05 rad. elevator step produced $u_{ss} = .246$ in the A4D-2, and $u_{ss} = 6.15$ in the modified Navion. As noted in the Appendix, the latter is well beyond the small perturbation theory employed in this investigation. Examination of the individual stability derivatives involved in the steady state transfer functions showed why the steady-state values differed so markedly between the two aircraft. Numerator terms causing the difference include $C_{m_{\delta_e}}$ and C_{L_α}, and a denominator

term, C_L, further complicated the picture. For example, $C_{m_{\delta_e}}$ of the Navion is approximately four and one-half times the value of that of the A4D-2; C_{L_α} of the Navion is about twice that of the A4D-2; and in the denominator, C_L of the Navion is about half that of the A4D-2. When these parameters are multiplied together, as is done in the transfer function, the steady-state value of u of the Navion, considering an equal amount of elevator step input, should be approximately 20 times that of the A4D-2. It should be emphasized that the principal offender in the steady-state transfer functions is the derivative $C_{m_{\delta_e}}$. In general, the same comments apply to the other perturbation quantities, α, $\dot{\theta}$ and θ, to varying degree. The above results were verified by computer studies and are tabulated in Table I.

As mentioned in EQUIPMENT AND PROCEDURE, computer studies were also made of the dynamic characteristics of the A4D-2, the Navion, and the modified Navion. Dynamic characteristics such as frequency and damping of the oscillatory modes peculiar to the "three" airplanes are also listed in Table I, and generally good agreement may be seen, except in the case of frequency and damping of the short periods; accuracy in the determination of short period characteristics from a time history trace is difficult at best. Fig. B1 shows the computer wiring diagram used in the computer simulation of the A4D-2, and it may be noted that it is a true representation of the type of feed-back system used in the Navion variable-stability installation.

Results of these computer studies also included transient values of the dynamic responses u, α, $\dot{\theta}$ and θ, for both the A4D-2 and the modified Navion. These results are also tabulated in Table 1. It may be noted

that the initial amplitudes of the response quantities to an elevator step forcing function of magnitude .05 rad. appear reasonable for the A4D-2, including normal acceleration(g's), but such quantities for the modified Navion are not only markedly different, but are well out of the realm of the small perturbation theory, as was true in the case of steady-state values. For the above reason, emphasis was shifted to the use of an impulse forcing function; as may be seen in Table I, however, even a .05 rad. impulse forcing function produced large initial amplitudes in oscillations of the response quantities, including 3.2 to 4.0 g's during the short period mode.

In order to determine the cause of such large differences between the two aircraft in amplitudes of oscillations of the response quantities, the airplane transfer functions were again examined, with emphasis this time on transient response. This procedure is also outlined in Appendix B. Examination of the transfer function $\frac{u}{\delta_e}(S)$ showed that the gain of the transfer function is composed of, in the numerator, $C_{m_{\delta_e}}$ and C_{D_α}, and in the denominator, a constant 2, h, and μ^3. Evaluation of the gain showed that $C_{m_{\delta_e}}$ and μ were the main causes of the large difference in gain between the A4D-2 and the modified Navion, viz., the gain of the Navion was about four times that of the A4D-2. Examination of the transfer function $\frac{\alpha}{\delta_e}(S)$ showed that the gain of the modified Navion was approximately seven times that of the A4D-2, and to further complicate the picture, the damping ratio of the second order lead term of the numerator of the Navion transfer function is approximately one-third that of the A4D-2, and well below critical damping. These factors appreciably altered amplitudes of response.

Then it may be seen that $C_{m_{\delta_e}}$ again altered desired response characteristics of the modified Navion, and additionally, the terms h and γ took part in this alteration. Examination of these terms and others will now follow, and later sections will touch on the same subject. It may be noted that a reduction of the magnitude of the elevator step or impulse will reduce the amplitude of oscillations of the response quantities of the modified Navion, and such reduction is linear with decrease in size of the step or impulse. However, there is some lower limit to this type of reduction; from the previous section it may be seen that the .05 rad. elevator step, for example, should be reduced by a factor of about 20 to $.14^{\circ}$. Examination of this from a practical standpoint, considering cable slop and resolution of the average auto-pilot, shows that this is the right direction but the wrong path.

Examination of the effects of $C_{m_{\delta_e}}$ indicates that if $C_{m_{\delta_e}}$ could be reduced, response characteristics would be improved; a solution in this direction would entail a small, auxiliary surface to be used as a moment-changer vice the Navion elevator. This will be discussed in more detail in a later section. Reduction of the amplitudes of the oscillations could be effected by increasing the magnitudes of h and γ ; this would indicate that the airplane to be simulated should have approximately the same mass and the same moment of inertia characteristics about the Y-axis as does the simulator airplane. It may be shown, however, that with a $\ddot{\theta}$ feed-back, moment of inertia characteristics may also be simulated. Then, in the general case, γ should be made approximately equal to that of the simulated aircraft.

In the last direction indicated above, that of using a light airplane to simulate a light airplane, resolution of the auto-pilot again becomes part of the picture. This phase was also investigated, and as

was expected, in the case that the aircraft and simulator aircraft are much alike in terms of stability derivatives and mass characteristics, the gain constants, $K_1 \ldots K_4$, tend to become extremely small; then the required magnitudes of the gain constants would tax an auto-pilot which had resolution approaching infinity -- or characteristics of a pure analog computer.

Because of the above, and other effects outlined in following sections, and the very limited time remaining for further investigation, emphasis was shifted to the secondary objective mentioned previously: a qualitative investigation of the effects of variation of the feed-back quantities. This was accomplished by means of root locii plots and was verified by computer studies. Only feed-backs of the algebraic sign designed for the A4D-2 were studied. Details of the root locii plots may be seen in Appendix B, and the general effects of the feed-back quantities are summarized in Table II. General comments concerning these effects are as follows: the principal effect of feeding-back angle of attack is to cause the frequency of the short period mode to decrease and the mode tends to become a convergent, aperiodic motion; there is little effect on damping of the short period, and frequency and damping of the phugoid.

Feeding back pitch-rate has the effect of altering dynamic characteristics of both the short period and phugoid modes; at very high gain, the frequency and damping of the short period mode decrease, and the mode tends to become aperiodic, convergent. Further, at low gain the damping and frequency of the phugoid increase, at some medium gain the damping decreases and the phugoid becomes oscillatory and divergent, and for very high gain the phugoid becomes aperiodic and divergent.

Unlike angle of attack, the velocity feed-back has the principal effect on the phugoid. For small gain, the frequency of the phugoid decreases, damping remains about constant, and the phugoid tends to become aperiodic, convergent. With another small increase in gain, the phugoid becomes aperiodic, divergent; further increase in gain results in greater divergence. In contrast, the damping and frequency of the short period mode are in general only somewhat increased.

The pitch angle feed-back, the only feed-back designed for stabilizing the motions of the modified Navion, also has a strong effect on the phugoid. At low gain, the frequency of the phugoid decreases and the damping increases until the motion becomes aperiodic, convergent. The short period is effected also, since the frequency increases and the damping decreases; this is again a small effect, however, as in the case of velocity feed-back.

Although limited time did not permit an investigation of the effects of the feed-backs taken simultaneously, at the magnitudes designed for the A4D-2 the separate effects of the feed-backs may be qualitatively summarized as follows: velocity and pitch angle feed-backs decreased the frequency of the phugoid of the Navion, thereby changing the frequency to that of the A4D-2 phugoid. The angle of attack feed-back was used to decrease the frequency and pitch-rate was used to decrease the damping of the short period. Finally, both pitch angle and pitch-rate were used to increase the damping of the phugoid.

FLIGHT TEST RESULTS

As noted in the section on EQUIPMENT AND PROCEDURE, the in-flight simulation of the A4D-2 was not attempted; some of the reasons therefor

are outlined in the preceding section. Flight testing that was done consisted of individual variations of the feed-back gains, also as mentioned previously. Although the aircraft, the variable-stability installation, the telemetering station, and associated equipment, were thought to be in good working order at the time of the test flight, numerous difficulties led to completely unsatisfactory flight test data.

Problems that arose with the Navion may be enumerated as follows: during flight testing of the phugoid mode, it was noticed that engine speed varied approximately 150 r.p.m. between high and low speeds of the phugoid. It was felt at that time that the added moment from change of thrust was causing an alteration of the dynamic characteristics of the phugoid. This was particularly noticeable in the testing of the effects of the feed-back u; for a small elevator impulse, with resultant small amplitudes of oscillations of attitude and airspeed, and with resultant small changes in engine r.p.m., the phugoid was a stable oscillatory motion. At the same feed-back gain setting, however, and with a larger elevator impulse, the phugoid became an unstable oscillation, during which time the engine r.p.m. changed considerably.

Another problem encountered with the Navion was the difficulty involved in trimming the aircraft prior to each test run. It had been found on a previous test flight that the auto-pilot trimming circuit was entirely too sensitive and could not be used to accurately trim the aircraft longitudinally. Since too little time then remained for changes of trim sensitivity, it was decided that the aircraft would have to be re-trimmed with the ship's elevator trimming system between each run of the test

flight with the auto-pilot disengaged. This was done during the test flight, but this method did not provide the cure: the Navion trimming system was also found to be very sensitive, and, in addition, manifold pressure required to fly the aircraft at the test speed in a level configuration varied by as much as four inches of mercury. The source of this additional trouble was not found. This difficulty in assuming the trimmed configuration naturally affected the phugoid test results.

As will be discussed later, the sensitivity of the pitch channel servo amplifier had to be reduced to prevent oscillation or cycling of the elevator at the flight test gain potentiometer settings (feed-back gains). This reduced the resolution of the elevator servo. The low resolution of the elevator servo was evident during the tests of the $\dot{\theta}$ feed-back; at low amplitudes of oscillation, there appeared to be little response from the elevator servo. During larger amplitudes of oscillation, the elevator was being moved in what was felt by the test pilot to be rather large steps, as indicated by somewhat rough control of the aircraft by the auto-pilot and seemingly large step-type changes in attitude.

Additionally, some turbulence was encountered at the test altitude, and attempts were made to avoid flying over freshly plowed fields, and the like. Also, communications proved to be unsatisfactory, despite the use of a communications relay station between the Navion and the telemetering station. Finally, considerable "drop-out" of the telemetered signal was encountered at the telemetering station.

The result of the above was unsatisfactory flight test data, and there was no time left for repeated testing.

THE VARIABLE-STABILITY INSTALLATION

The variable-stability installation was built around a three-channel auto-pilot, which in turn consists essentially of three servo amplifiers and three servo motors used to position the control surfaces. The electric stick is used to generate voltage signals, these signals are summed with voltage signals from aircraft attitude and rate sensors, and the resulting voltage causes the servo motors to position the control surfaces. The installation is pictured schematically in Fig. 1. Considering the longitudinal channel, the servo motor positions the elevator through a bridle fastened to the ship's elevator cables, as may be seen in the schematic drawing, Fig. 2. Also, since the various sensors and the electric stick are excited by a.c. transformers, the signals generated have both magnitude and sense.

The gain potentiometers provided are used to divide the sensor signal voltages, and the portions of the sensor signal voltages summed and fed to the amplifier are dictated by the gain pot settings. The gain pot settings, in turn, are a function of required gain constants. The algebraic signs of the gain constants are determined by the polarity of the exciting transformer, e.g., for the A4D-2 simulation, polarity such that down elevator results from an increase in u.

In addition, a trim circuit was installed. The trim circuit provides a voltage of magnitude equal to but of phase opposite to summed voltages from the sensors, thereby permitting auto-pilot engagement.

To illustrate the elevator-movement sequence, assume that the initial input is a voltage generated by stick deflection. The servo and bridle move the elevator until the servo follow-up circuit generates a signal equal in magnitude and opposite in phase to the stick input signal. As the aircraft responds to the elevator deflection, voltages are generated by the pitch gyro, pitch-rate gyro, airspeed transducer, and angle of attack vane. These voltages, after being summed in the pitch channel summing circuit, as may be seen in Fig. 3, are fed through the servo amplifier to the servo motor, which deflects the elevator. The elevator augments or damps the aircraft response, depending on the phase of the summed a.c. voltage fed to the servo motor.

A detailed description of the variable-stability installation is contained in Appendix C, including pictures of the installation, descriptions of the structural and electrical components, and graphs of the control cable forces which were the basis of the structural design.

Safety features of the auto-pilot consist of the following devices: an auto-pilot disengage switch is provided on the left console of the cockpit for the safety-pilot, and a disengage button is provided on the electric stick for the test pilot. In addition, an electrical cut-off device is provided. If a large error signal is received at the point of input to the servo amplifiers, an electrical device breaks the circuit to the servos, thereby disengaging the auto-pilot. When this occurs, another device disengages completely the gearing between the servo motor and the servo pulley; the pulley then rotates freely on bearings only. Finally, as noted previously, servo clutches may be caused to slip, i.e., the

safety-pilot may manually override the servo motors with the ship's controls.

Structurally, the auto-pilot variable-stability installation was found to be satisfactory in all respects except for cable slop in the aileron system. Some bending of the aileron servo cable pulley brackets was discovered during the static tests; this bending resulted in aileron cable slack at very high control force conditions. These pulleys and pulley brackets were the original ones used in the Navion aileron follow-up system, and because of position, the brackets were not readily accessible for structural stiffening.

AUTO-PILOT LIMITATIONS

As mentioned previously, the gain constants required for the simulation were found to be of such magnitude that, for example, the auto-pilot had to be designed to furnish about $.6^{\circ}$ of elevator deflection for a 15° change in angle of attack. Considering excitation voltage on the servo motor(corresponding to about 4° of elevator travel per volt), for a 15° change in angle of attack, the resulting voltage (from the angle of attack vane) which was fed into the summing circuit was about .12 volts. The other gain constants, in general, resulted in similar magnitudes of voltages, with the exception of the pitch angle gain constant, which was an order of magnitude smaller. In order to provide such magnitudes of voltages, with the available sensor excitation voltages ($\pm$ 7.5 to $\pm$ 30 volts), and in order to provide gain potentiometer settings that were reasonable (towards the middle of the pot indicator scales), 15,000 to 500,000 ohm end-resistors had to be installed in the individual sensor

circuits in series with the gain potentiometers. (For comparison, gain potentiometers and sensor potentiometers have resistances of approximately 5000 ohms.)

In a chain type reaction, considerable quadrature was produced in the summing circuit, the trimming circuit could not "interpret" the phase shift of the voltage, with the result that the voltage in the summing circuit could not be zeroed, and the auto-pilot could not be engaged. Quadrature was forthwith adjusted, the auto-pilot was engaged, but with any change of gain pot setting or sensor position, the electric cut-out disengaged the auto-pilot. Quadrature, then, was found to be a function of not only pot settings, but sensor positions as well. In addition, as indicated, the electric cut-out could not "distinguish" quadrature from a large error signal.

To relieve the above situation, the emphasis had to be shifted to the second objective, investigation of the effects of variations of single feed-backs. The end-resistors were removed, but some quadrature effects were still found to be present. It was found that, for example, as the angle of the angle of attack vane was changed, a small amount of phase shift still took place; the explanation was that with the change of resistance of the angle of attack pot (associated with movement of the vane) came also a change in a.c. impedance, causing phase shift.

To relieve this same situation, and to thereby permit flight-testing, the cut-out circuit had to be adjusted to a much less sensitive level, and the sensitivity of the servo amplifier had to be decreased to prevent cycling of the servo motor. The reduction of sensitivity of the servo

amplifier reduced the resolution of the servo motor. The result was a barely acceptable longitudinal auto-pilot, considering the small changes of aircraft response which occur, for instance, during the phugoid mode.

To further complicate the picture, the only suitable pressure (air-speed) transducer that could be located during auto-pilot installation had a non-linear potentiometer. This could be an additional explanation for aircraft-auto-pilot behavior during flight testing.

As mentioned previously, auto-pilot resolution was an additional problem. Initially, resolution of the auto-pilot amounted to approximately $\pm .5^{\circ}$, i.e., the auto-pilot could position the elevator within one-half degree of the commanded deflection. This resolution was found to be a function of the excitation voltage on the servo motor, and the magnitude of the signal voltage required to close the servo relay circuit. To improve resolution, the excitation voltage on the servo motor was increased to the maximum available in the system, ± 30 volts. In addition, the peck-size of the relay was decreased with use of the servo-amplifier throttling control, or in other words, the amount of time that the relay remained closed was decreased. This effectively increased the peck-rate of the relay. These two improvements increased the resolution to about $\pm 1/4^{\circ}$. In an attempt to further increase resolution, a high-frequency sinusoidal voltage was superimposed on the relay, or, the "dithering" process. The result was unsatisfactory in that the elevator cycled at some sub-harmonic of the dither frequency. Finally, the sensitivity of the servo amplifier had to be reduced to prevent cycling of the servo motor, which was believed to be induced by electrical noise

in the system; this reduced the resolution of the auto-pilot, but an absolute value of the resolution was not thereafter obtained. However, considering the $.05^{\circ}$ of elevator required by the θ feed-back in particular, it may be seen that even the improved resolution is an order of magnitude less than that required.

In summary, the resolution and the quadrature problems were additional indications that a small, auxiliary surface should be used as the moment-changer, instead of the Navion elevator. In such a case, voltages would have been much larger, and quadrature problems of such magnitude could have been avoided. Another approach would have been to design the auto-pilot variable-stability system for d.c. summing circuit operation rather than a.c.

CALIBRATIONS

Quadrature also affected calibrations. With the end-resistors in place in the sensor circuits, for accuracy, quadrature had to be constantly adjusted during calibration for each range of pot settings. In addition, the sensor output voltages, as measured in the summing circuit, were so small that "they" could not be measured accurately with the existing voltmeters; this necessitated the removal of the end-resistors, calibration with other much smaller end-resistors, and a proportionate scaling of the calibrated quantities. Final calibrations may be seen in Appendix C; they are approximate for no end-resistors in place in the sensor circuits.

WEIGHT AND BALANCE LIMITATIONS

According to the Navion Operator's Handbook, maximum permissable weight is 2750 lbs., and maximum C.G. position is 30.5% of M.A.C., gear down. With

loaded configuration, including two pilots, full fuel load, and no passengers, the variable-stability Navion weighs 2750 lbs., and with gear down, the C.G. is 29.5% of M.A.C.

ADDITIONAL DISCUSSION

In summary, it has been shown in the preceding sections and in the Appendices, that with the Navion variable-stability installation, only the Navion moment equation was altered, not the lift or the drag equations. Further, provisions were made only for modifying two stability derivatives of the moment equation, C_{m_α} and $C_{m_{d\theta}}$, and for the addition of two pseudo-derivatives to the moment equation, C_{m_u} and C_{m_θ}. It has been seen that with such changes of the Navion moment equation, the characteristic equation of the A4D-2 could be simulated, as was verified by use of the analog computer. Such simulation meant that the longitudinal dynamic characteristics damping and frequency of both modes of motion could be simulated. As was shown later, however, steady-state values and amplitudes of oscillations of the airplane responses could not be simulated. This last, coupled with auto-pilot quadrature and resolution problems, led to the abandonment of the simulation.

Although the Navion variable-stability installation has a number of problems in the longitudinal channel, this does not detract from the value of variable-stability installations in general. The literature contains the results of many successful installations, and the real value of such an installation is the fact that artificial control permits changes in the stability characteristics of the test aircraft while the aircraft is airborne. Without artificial control, it is impossible

to modify existing stability derivatives of a given airplane without major and costly structural changes. At the same time, without artificial control, it is impossible to add new and additional stability derivatives, other than those normally contained in the three equations of motion, since there is no choice of what the airplane can "sense."

With the variable-stability auto-pilot, the outputs of many types of sensing devices can be used, and there are practically endless possibilities in this direction, according to the literature, including Ref. 15. For example, in Ref. 4, the investigators used α and $\dot{\alpha}$ feed-backs to modify only the characteristics of the short period mode of the test aircraft; these response feed-backs were used in order not to appreciably change the phugoid. Also, u and $\dot{u}$ feed-backs have been used to only modify the phugoid response. As has been discussed in the present report, α and u feed-backs actually do just what is indicated above, and a quick examination of the root locii plots will show that $\dot{\alpha}$ and $\dot{u}$ also have the effects described above.

Another approach to the variable-stability installation theory might be changes of the other two equations of motion, lift and drag, although this is not believed to be as practical as the moment-changer version.

Also as indicated in the literature (see Ref. 4), the small, auxiliary surface as a moment-changer is a practical appendage of the variable-stability installation. This has been verified by the results indicated in the present report. Instead of using a very powerful tool such as the Navion elevator to modify aircraft responses, it has been suggested, for conjecture, that the elevator trim tab could be used as the moment-changer.

Unfortunately, in the case of the Navion installation, this would mean additional weight for an additional servo motor, and other auto-pilot components, and it has been seen that maximum weight and C.G. conditions presently exist.

CONCLUSIONS

In view of the previous, it is concluded that:

1) Simulation of the longitudinal flight motions of other aircraft cannot be successfully accomplished with the present Navion variable-stability installation.

2) Considering simulation in general, unless all three equations of motion can be modified, steady-state values of aircraft responses and amplitudes of oscillations of responses cannot be exactly simulated; however, characteristic equations and thus dynamic response characteristics such as frequency and damping of the aircraft modes can be simulated.

   a) Considering gains of the airplane transfer functions, and auto-pilot resolution, a small, auxiliary surface should be used as the moment-changer in such type of variable-stability installation. Also, the test aircraft should have room for weight growth.

   b) Considering gains and numerator terms of the airplane transfer functions, in general, the simulator aircraft should have approximately the same time constant, τ , as does the aircraft which is to be simulated.

3) In the present configuration the Navion is not suitable for in-flight testing of the effects of airplane longitudinal response feed-backs.

4) Concerning feed-back quantities, α has a primary effect on the short period mode, u and θ have primary effects on the phugoid, and $\dot{\theta}$ has effect on both the short period and the phugoid modes.

RECOMMENDATION

Considering present Navion weight, present C.G. location, longitudinal auto-pilot limitations, and engine (r.p.m.) characteristics, it is recommended that future investigations with the Navion variable-stability installation be limited to lateral-directional flight testing.

BIBLIOGRAPHY

1. Sjoherg, S.A., Russell, W.R., and Alford, W.A.: A Flight Investigation of the Handling Characteristics of a Fighter Airplane Through an Attitude Type of Automatic Pilot. NACA RM L56A12, 1956

2. Ciscel, Benitti: Control Stick Steering for Stabilized Aircraft. Aer. Eng. Rev., Vol. 14, No. 1, January 1955.

3. Kidd, E.A., and Gould, A.: An Artificial Stability Installation in a C-45 Airplane. Cornell Aeronautical Laboratory Report No. TB-754-F-2, July 1953.

4. Chalk, C.R.: Additional Flight Evaluations of Various Longitudinal Handling Qualities in a Variable-Stability Jet Fighter. WADC Technical Report 57-719, Part I, January 1958.

5. Kauffman, W.M., Smith, A., et al.: Flight Tests of an Apparatus for Varying Dihedral Effect in Flight. NACA TN 1788, December 1948.

6. Kidd, E.A.: Artificial Stability Installation in B-26 and F-94 Aircraft. WADC TR 54-441, October 1954.

7. Brissendon, R.F., Albord, W.L., and Mallic, D.L.: Flight Investigation of a Pilot's Ability to Control an Airplane Having Positive and Negative Static Longitudinal Stability Coupled with Various Effective Lift-Curve Slopes. NASA TN D-211, 1960.

8. Brenhaus, W.O.: Flight Research Utilizing Variable Stability Aircraft. Aero Eng. Rev., Vol. 14, No. 11, November 1955.

9. O'Hara, J.F., and Ebbert, E.L.: A Preliminary Evaluation of the Navion as a Lateral-Directional Flight Simulator for Use in the Investigation of Flying Qualities Criteria. Aeronautical Engineering Report No. 509 Princeton University, May 1960.

10. Perkins, C.D., and Hage, R.E.: Airplane Performance, Stability, and Control. John Wiley and Sons, Inc., New York, 1958.

11. Schuld, E.P. and Reinhart, L.J.: Determination of Longitudinal Stability Parameters by Steady State Flight Testing and Theoretical Calculations for the Ryan Navion. Aeronautical Engineering Report No. 232, Princeton University, June 1953.

12. Drake, D.E., Keown, E.R., and Matlock, J.K.: Programming of Digital Computers for Determination of Stability and Control Characteristics. Vol. IV and V, WADC TR 59-290, July 1, 1959

BIBLIOGRAPHY (continued)

13. Stability and Control (Flight Phase) Manual. Naval Air Test Center Report, Patuxent River, 30 June 1953.

14. Pilot Techniques for Stability and Control Testing. Naval Air Test Center, Patuxent River, 15 March 1955.

15. Milliken, W.F., Jr.: Dynamic Stability and Control Research. Cornell Aero. Lab., Inc., Report CAL-39, September 3-14, 1951.

TABLE I

DYNAMIC RESPONSE SUMMARY

CONFIGURATION	PERIOD, DAMPING				TRANSIENT VALUES (2,3,7)						STEADY-STATE VALUES (3,6)		
	Short Period		Phugoid		δ_e° (5)	u	α°_{sp}	$\dot{\alpha}_{phu}$	θ°	n_z	u	α°	θ°
	$T_{\frac{1}{2}}$	P	$T_{\frac{1}{2}}$	P									
NAVION	.26 (1)	3.78	62.6	32.9									
	-- (2)	--	62.0	31.5									
A4D-2	.94 (1)	6.59	39.5	34.9		-.45	5.5	7.8	19.5	1.5	-.246	6.45	3.95
	-- (2)	--	40.0	35.0									
MODIFIED NAVION	.94 (1)	6.59	39.5	34.9		-10.0	83			6.8	-6.15	63	77
	-- (2)	--	39.0	35.5	12 (4)	-.75	16	4		3.2 - 4.0			

1. Factored equations, or other analytical
2. Computer
3. .05 rad. δ_e step
4. .05 rad. δ_e impulse
5. Includes feedbacks
6. Analytical, and verified by computer
7. Amplitude of first oscillation

TABLE II

FEEDBACK SUMMARY

INCREASING (1)	INCREASES	DECREASES	BECOMES			HAS PRINCIPAL EFFECT ON
			Divergent, Oscillatory	Convergent, Aperiodic	Divergent, Aperiodic	
K_1 (α)	P_{sp}			Short Period		Short Period
K_2 $(\dot{\theta})$	P_{sp}, $T_{\frac{1}{2}sp}$	P_{phu}, $T_{\frac{1}{2}phu}$	Phugoid (2)	Short Period		Both
K_3 (u)	P_{phu}	P_{sp}, $T_{\frac{1}{2}sp}$			Phugoid	Phugoid
K_4 (θ)	P_{phu}, $T_{\frac{1}{2}sp}$	P_{sp}, $T_{\frac{1}{2}phu}$		Phugoid		Phugoid

1. Sign of feedback as designed for A4D-2, with the Navion as the simulation vehicle.
2. At high gain.
3. Code: P_{phu} - period of phugoid mode

   P_{sp} - period of short period mode

   $T_{\frac{1}{2}phu}$ - time to damp to $\frac{1}{2}$ amplitude, phugoid

   $T_{\frac{1}{2}sp}$ - time to damp to $\frac{1}{2}$ amplitude, short period

TABLE III

NAVION SPECIFICATIONS

Model	North American Navion
Length	27.25 ft.
Wing Span	33.36 ft.
Wing Area	184.2 ft.^{2}
Gross Wt.	2750 lbs.
C.G. Position	29.5% M.A.C. (with Auto-pilot)
Power Plant	Continental, six cylinder, horizontal-opposed, 205 HP
Propeller	Hartzell, variable pitch, constant speed
Landing Gear	Tricycle, retractable

FIGURE 1

PITCH CHANNEL AUTO-PILOT

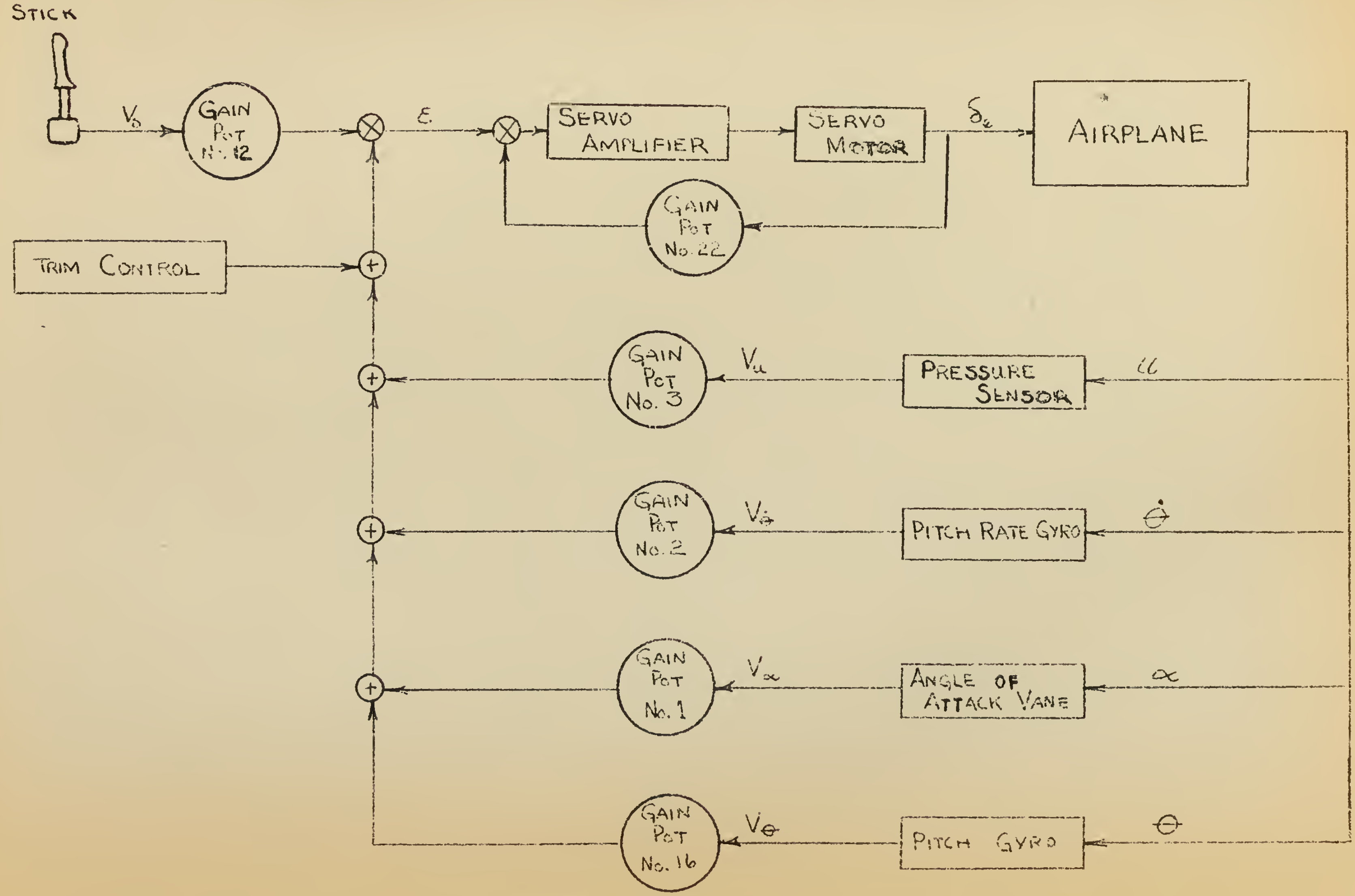

FIGURE 2

CONTROL SYSTEM SCHEMATIC

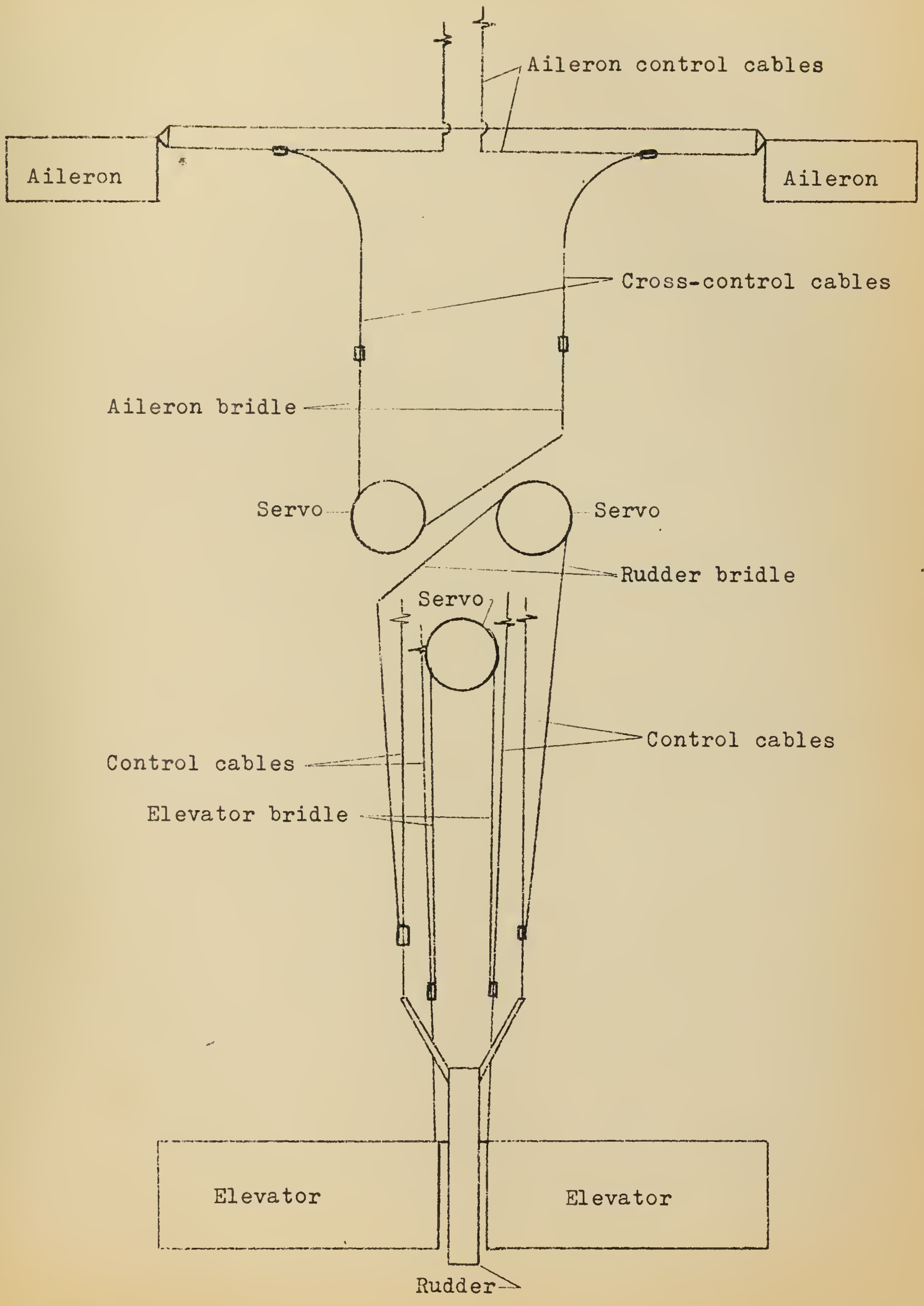

FIGURE 3

PITCH CHANNEL SUMMING CIRCUIT

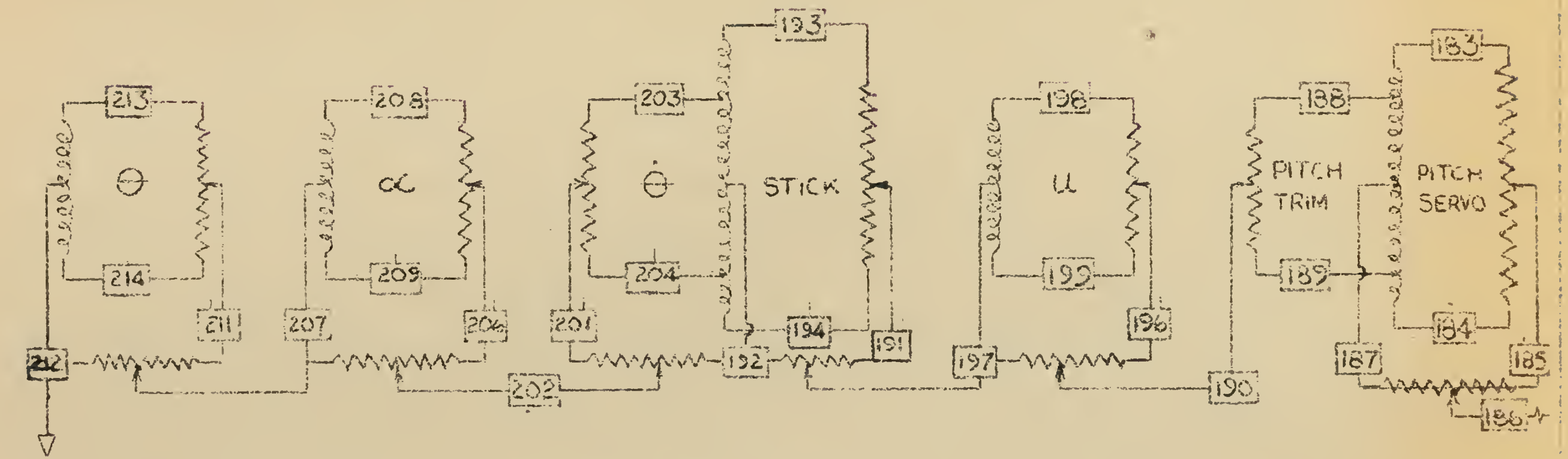

Gain Pot	16	1	2	12	3		22
Transformer Winding	12	18	16	16	2 and ½ of 10	½ of 1 and ½ of 4	4 and 1
Voltage	±7.5	±7.5	±7.5	±15	±27.5	±15	±30
Telemeter Channel	7	4	6	10	8		

☐ - Terminal number

☐ - Terminal number, telemeter a.c. voltage

APPENDIX A

THEORY AND ANALYSIS

MODIFIED NAVION DERIVATIVES AND EQUATIONS

Given conditions: Clean configuration, power on (1850 rpm)

$h = 6500$ ft., $\rho = .001957$ slugs/ft.^{3}

$V_o = 120$ mph $= 176$ ft./sec.

From Ref. 11 : $N_o = .384$ (Neutral Point)

$C_{L_\alpha} \doteq .095$/deg. $= 5.45$/rad.

$C_{m_{\delta_e}} = -\ .025$/deg. $= -1.435$/rad.

$C_{m_{d\theta}} = -\ .15$/rad. $(I_Y)_{jig} = 3055$ slug ft.^{2}

$C_{m_{d\alpha}} = -\ .07$/rad.

Assumption : That the derivatives above, which are for the Ryan Navion, may be applied also to the North American Navion; both airplanes are standard "blueprint copies" made by two different aircraft companies.

Calculations :

C_{m_α} : $C_{m_\alpha} = C_{L_\alpha}\ (X_{CG} - N_o) = 5.45(.295 - .384)$

$= -\ .485$/rad.

W/S : W/S $= 2750/184.2 = 14.93$ lbs./ft.^{2}

C_{L_o} : $C_{L_o} = \dfrac{W/S}{q} = \dfrac{14.93}{1/2(.001957)(176)^2} \doteq .493$

C_{D_α} : $C_{D_\alpha} \doteq \dfrac{2C_{L_o}\ C_{L_\alpha}}{\pi A_e} \doteq \dfrac{2(.493)\ 5.45}{\pi\ (6.04)\ .85} = .333$/rad.

Calculations :

C_{D_o} : $$C_{D_o} \doteq C_{D_f} + \frac{C_L^2}{\pi A_e} \doteq .025 + \frac{(.493)^2}{\pi(6.04).85} = .0401$$

τ : $$\tau = \frac{m}{\rho SV} = \frac{2750}{32.17(.001957)(176)(184.2)} = 1.35 \text{ sec.}$$

μ : $$\mu = \frac{m}{\rho S \bar{c}} = \frac{85.5}{.001957(184.2)5.7} = 41.6$$

$I_{Y_{CG}}$: $$I_{Y_{CG}} = I_{Y_{jig}} - mr^2$$
$$= 3055 - 85.5(1.39)^2 \doteq 2890 \text{ slug ft.}^2$$

K_y^2 : $$K_y^2 = \frac{I_Y}{m} = \frac{2890}{85.5} = 33.8 \text{ ft.}^2$$

h : $$h = \frac{2}{\mu} \frac{K_y^2}{\bar{c}^2} = \frac{2}{41.7} \cdot \frac{33.8}{(5.7)^2} = .05$$

C_{m_u} : $$C_{m_u} \doteq 0$$

$C_{D_{eff}}$: $$C_{D_{eff}} \doteq C_{D_o}$$

$C_{L_{eff}}$: $$C_{L_{eff}} \doteq C_{L_o}$$

Characteristic equation, Modified Navion: Dividing all coefficients by $- h \tau^4$:

$$C_4 \lambda^4 + C_3 \lambda^3 + C_2 \lambda^2 + C_1 \lambda + C_o = 0$$

where $C_4 = 1$

$$C_3 = \frac{-1}{h \tau} \left[C_{m_{d\theta}} \; G_2 + C_{m_{d\alpha}} - h\left(\frac{C_{L_\alpha}}{2} + C_{D_{eff}}\right) \right]$$

$$= \frac{-1}{.05(1.35)} \left[- .15 \; G_2 - .07 - .05(2.725 + .0401) \right]$$

$$= 5.30 + 15.75 \; K_2$$

$$C_2 = \frac{1}{-h\rho}2 \Bigg[C_{D_{eff}}(C_{m_{d\alpha}} + C_{m_{d\theta}}G_2 - \frac{hC_L}{2}{}_{\alpha}) + \frac{hC}{2}{}_{L_{eff}}(C_{D_\alpha} - C_L)$$

$$+ \frac{C_L}{2}{}_{\alpha}(C_{m_{d\theta}}G_2) + C_{m_\alpha} G_1 + K_4C_{m_{\delta_e}}\Bigg]$$

$$= \frac{-1}{.050(1.822)} \Bigg[.0401\Big\{ - .07 - .15G_2 - .05(2.725)\Big\}$$

$$+ \frac{.05(.493)}{2} (.333 - .493) + 2.725(- .15G_2\Big\} - .485G_1$$

$$- 1.435K_4\Bigg]$$

$$= 9.88 + 15.74K_1 + 32.27K_2 + 15.73K_4$$

$$C_1 = \frac{1}{-h\rho}3 \Bigg[C_{D_{eff}}(\frac{C_{L_\alpha}}{2} C_{m_{d\theta}}G_2 + C_{m_\alpha} G_1) + \frac{C_L\ C}{2}{}_{L_{eff}}(C_{m_{d\theta}} G_2$$

$$+ C_{m_{d\alpha}} - \frac{C_{D_\alpha}}{C_L} C_{m_{d\theta}} G_2) - \frac{C_{m_u}}{2} G_3C_{D_\alpha} + K_4C_{m_{\delta e}}(C_{D_{eff}} + \frac{C_L}{2}{}_{\alpha})\Bigg]$$

$$= \frac{-1}{.05(2.46)} \Bigg[.0401\Big\{2.725(-.15)G_2 - .485G_1\Big\} + (\frac{.493}{2})^2 \Big\{-.15G_2$$

$$- .07 - \frac{.333}{.493} (- .15)G_2\Big\} - \frac{C_{mu}}{2} (.333)G_3 - 1.435K_4(.0401+2.725)\Bigg]$$

$$= .408 + .468K_1 + 1.284K_2 - 1.942K_3 + 32.25K_4$$

$$C_o = \frac{1}{-h\rho}4 \Bigg\{\frac{C_L}{2} \Big[C_{L_{eff}}C_{m_\alpha} G_1 - \frac{C_L}{2}{}_{\alpha}C_{m_u}G_3\Big] + K_4C_{m_{\delta_e}}\Big[C_{D_{eff}} \frac{C_L}{2}{}_{\alpha}$$

$$- \frac{C}{2}{}_{L_{eff}}(C_{D_\alpha} - C_L)\Big]\Bigg\}$$

$$= \frac{-.493}{2(.05)3.32} \Big[-.493(.485)G_1 - 2.725\ C_{m_u}G_3\Big]$$

$$+ \frac{1.435K_4}{(.05)3.32} \Big[(.0401)2.725 - \frac{.493}{2}(.333 - .493)\Big]$$

$$= .355 + 1.051\ K_1 - 5.81\ K_3 + 1.285\ K_4$$

A4D-2 DERIVATIVES AND EQUATIONS

From Ref. 12, the A4D-2 derivatives are as follows:

Given conditions: Clean configuration, power on

$h = 6500$ ft. V_o = Mach .2 = 218 ft./sec.

From Ref. 12:

$C_{L_\alpha} = 3.62$/rad.

$C_{m_{\delta e}} = -.3265$/rad.

$C_{m_\alpha} = -.145$/rad.

$C_{m_{D\alpha}} = -1.090\text{/rad.} = \left[\dfrac{\partial C_m}{\partial(\dot{\alpha}\frac{\bar{c}}{2V})}\right]$

$C_{m_q} = -3.263\text{/rad.} = \left[\dfrac{\partial C_m}{\partial(\frac{q\bar{c}}{2V})}\right]$

$C_{m_u} = 0$

$I_Y = 17{,}600$ slug ft.^{2}, $S = 260$ ft.^{2}

$\bar{c} = 10.8$ ft., $W = 10{,}000$ lbs.

CG = 25% MAC, $b = 27.5$ ft.

Computation:

C_{L_o} :

$$C_{L_o} = \frac{W/S}{q} = \frac{10}{1/2(.001957)(218)^2 260} = .828$$

$$C_{D_{min}} \doteq .059, \quad e \doteq .572, \quad A = 2.91$$

C_{D_o} :

$$C_{D_o} \doteq C_{D_{min}} + \frac{(C_{\bar{L}})^2}{\pi A_e}$$

$$\doteq .059 + \frac{(.828)^2}{\pi 2.91(.572)} \doteq .190$$

C_{D_α} :

$$C_{D_\alpha} \doteq \frac{2C_L C_{L_\alpha}}{\pi A_e} = \frac{2(.828)3.62}{\pi(2.91).572} = 1.147\text{/rad.}$$

τ :

$$\tau = \frac{m}{\rho SV} = \frac{10{,}000/g}{.001957 \times 260 \times 218} = 2.81 \text{ sec.}$$

Computation:

$$C_{m_{d\alpha}} \quad : \quad C_{m_{d\alpha}} = C_{m_{D\alpha}} \cdot \frac{\bar{c}}{2V\tau} = \frac{-1.090(10.8)}{2(218)2.81} = -.00961/\text{rad.}$$

$$C_{m_{d\theta}} \quad : \quad C_{m_{d\theta}} = C_{m_q} \cdot \frac{\bar{c}}{2V\tau} = \frac{-3.263(10.8)}{2(218)2.81} = -.0288/\text{rad.}$$

$$K_y^2 \quad : \quad K_y^2 = \frac{I_y}{m} = \frac{17,600}{10,000/g} = 56.6 \text{ ft.}^2$$

$$\mu \quad : \quad \mu = \frac{m}{\rho S C} = \frac{10,000/g}{.001957(260)10.8} = 56.6$$

$$h \quad : \quad h = \frac{2}{\mu} \frac{K_y^2}{\bar{c}^2} = \frac{2}{56.6} \frac{(56.6)}{(10.8)^2} = .01715$$

Characteristic equation, A4D-2: Dividing all coefficients by $-h\tau^4$:

$$C_4' \lambda^4 + C_3' \lambda^3 + C_2' \lambda^2 + C_1' \lambda + C_o' = 0, \text{ where}$$

$$C_4' = 1$$

$$C_3' = \frac{-1}{h\tau}\left[-h\left(C_D + \frac{C_{L\alpha}}{2}\right) + C_{m_{d\alpha}} + C_{m_{d\theta}}\right]$$

$$= \frac{-1}{(.01715)(2.81)}\left[-.01715(.19 + 1.81) - .00961 - .0288\right] = 1.508$$

$$C_2' = \frac{-1}{h\tau^2}\left[h\left\{\frac{C_L}{2}(C_{D_\alpha} - C_L) - \frac{C_D C_{L\alpha}}{2}\right\} + C_D(C_{m_{d\alpha}} + C_{m_{d\theta}})\right.$$

$$\left. + \frac{C_{L\alpha}}{2} C_{m_{d\theta}} + C_{m_\alpha}\right]$$

$$= \frac{-1}{.01715(2.81)^2}\left[.01715\left\{.414(1.147 - .828) - .19(1.81)\right\}\right.$$

$$\left. + .19(-.00961 - .0288) + 1.81(-.0288) - .145\right]$$

$$= 1.536$$

$$C_1' = \frac{-1}{h\,\tau^3}\left[C_D\left(\frac{C_{L_\alpha}}{2}\,C_{m_{d\theta}} + C_{m_\alpha}\right) + \frac{C_L}{2}\left(C_L C_{m_{d\alpha}} - C_{m_{d\theta}}\left\{C_{D_\alpha} - C_L\right\}\right)\right]$$

$$= \frac{-1}{(.01715)(2.81)^3}\left[.19(1.81\times -.0288 - .145) + .414\left\{(.828)(-.00961) + .0288(.319)\right\}\right]$$

$$= .0968$$

$$C_0' = \frac{-C_L{}^2 C_{m_\alpha}}{2h\,\tau^4} = \frac{-(.828)^2(-.145)}{2(.01715)(2.81)^4} = .0464$$

GAIN CONSTANTS

Equating the constants of the two characteristic equations:

$$(C_4')_{A4D-2} = (C_4)_{MOD.NAV.} = 1$$

$$C_3' = 1.508 = 5.30 + 15.75K_2$$

$$C_2' = 1.536 = 9.88 + 15.74K_1 + 32.27K_2 + 15.73K_4$$

$$C_1' = .0968 = .408 + .468K_1 + 1.284K_2 - 1.942K_3 + 32.25K_4$$

$$C_0' = .0464 = .355 + 1.051K_1 - 5.81K_3 + 1.285K_4$$

Solutions of these equations yielded:

K_1 = - .0407, dimensionless

K_2 = - .240, sec.

K_3 = .0465, rad.

K_4 = .0033, dimensionless

APPENDIX B

ANALYTICAL STUDIES

COMPARISON OF DYNAMIC CHARACTERISTICS

Factorization of the characteristic equations yielded the following:

A4D-2, and MOD. NAV.:

Phugoid $\lambda^2 + .0351\lambda + .0325 = 0$

$\lambda_{phu} = - .01755 \pm .18i$

$T_{1/2} = 39.5$ sec. $P = 34.9$ sec.

Short Period $\lambda^2 + 1.473\lambda + 1.452 = 0$

$\lambda_{sp} = - .737 \pm .954i$

$T_{1/2} = .94$ sec. $P = 6.59$ sec.

NAVION:

Phugoid $\lambda^2 + .0212\lambda + .0366 = 0$

$T_{1/2} = 62.6$ sec. $P = 32.9$ sec.

Short Period $\lambda^2 + 5.28\lambda + 9.72 = 0$

$T_{1/2} = .26$ sec. $P = 3.78$ sec.

COMPARISON OF STEADY-STATE VALUES

The steady-state denominator term common to each aircraft transfer function:

$$\Delta_{s.s.} = \begin{vmatrix} C_{D_{eff}} & 1/2\,(C_{D_\alpha} - C_L) & C_L/2 \\ C_{L_{eff}} & \dfrac{C_{L_\alpha}}{2} & 0 \\ 0 & C_{m_\alpha} & 0 \end{vmatrix}$$

$$= \frac{C_L^2}{2} C_m$$

Steady-state numerator terms:

$$(N_u)_{s.s.} = \begin{vmatrix} 0 & 1/2(C_{D_\alpha} - C_L) & \frac{C_L}{2} \\ 0 & \frac{C_{L_\alpha}}{2} & 0 \\ -C_{m_{\delta_e}}\delta_e & C_{m_\alpha} & 0 \end{vmatrix}$$

$$= C_{m_{\delta_e}}\delta_e \frac{C_L}{4} C_{L_\alpha}$$

$$(N_\alpha)_{s.s.} = \begin{vmatrix} C_{D_{eff}} & 0 & C_L/2 \\ C_{L_{eff}} & 0 & 0 \\ 0 & -C_{m_{\delta_e}}\delta_e & 0 \end{vmatrix}$$

$$= -\frac{C_L^2}{2} C_{m_{\delta_e}}\delta_e$$

$$(N_\theta)_{s.s.} = \begin{vmatrix} C_{D_{eff}} & 1/2(C_{D_\alpha} - C_L) & 0 \\ C_{L_{eff}} & \frac{C_{L_\alpha}}{2} & 0 \\ 0 & C_{m_\alpha} & -C_{m_{\delta_e}}\delta_e \end{vmatrix}$$

$$= -C_{m_{\delta_e}}\delta_e \left[\frac{C_D C_{L_\alpha}}{2} - \frac{C_L}{2}(C_{D_\alpha} - C_L)\right]$$

A4D-2:

Evaluation of steady-state values for .05 rad. δ_e (down elevator) step forcing function yielded:

$u_{s.s.} = + .246$ [Computer: + .255]

$\alpha_{s.s.} = - .113$ rad. $= - 6.45^\circ$ [Computer: - .114 rad.]

$\theta_{s.s.} = - .069$ rad. $= - 3.95^\circ$ [Computer: - .070 rad.]

MODIFIED NAVION:

For the same forcing function as above (including feed-backs):

$u_{s.s.} = 6.15$ [Computer: 5.8]

$\alpha_{s.s.} = -1.1$ rad. [Computer: - 1.0 rad.]

$\theta_{s.s.} = -1.35$ rad. [Computer: - 1.3 rad.]

COMPUTER (DYNAMIC STUDY)

A4D-2: Computer equations:

Lift : $\dot{u} + \frac{C_D}{\tau} u + \frac{1}{2\tau}(C_{D_\alpha} - C_L)\alpha + \frac{C_L}{2\tau}\theta = 0$

Drag : $\dot{\alpha} + \frac{C_L}{\tau} u + \frac{C_{L_\alpha}}{2\tau}\alpha - \dot{\theta} = 0$

Moment : $\ddot{\theta} + \left(\frac{-C_{m_\alpha}}{h\tau^2}\right)\alpha + \left(\frac{-C_{m_{d\alpha}}}{h\tau}\right)\dot{\alpha} + \left(\frac{-C_{m_{d\theta}}}{h\tau}\right)\dot{\theta} + \left(\frac{-C_{m_{\delta_e}}}{h\tau^2}\right)\delta_e = 0$

Damping and Period:

Phugoid $T_{1/2} = 40.0$ sec., $P = 35.0$ sec.

Short Period $T_{1/2} \doteq .8$ sec., $P \doteq 8.0$ sec.

Transient values: For .05 rad. δ_e (up elevator) step input, amplitudes of initial oscillations are as follows:

$u = -.45$

$\alpha_{sp} = 5.5^\circ$

$\alpha_{phu} = 7.8^\circ$

$\theta = 19.5^\circ$

Transient normal acceleration:

$$W(n - 1) = \frac{W}{g} a$$

or $(n - 1)g = a = \frac{V^2}{R}$, and $\dot{\theta} = \frac{V}{R}$

then $\dot{\theta} = g\frac{(n - 1)}{V}$

or $n = \frac{V\dot{\theta}}{g} + 1$. From the computer,

$\dot{\theta} = .08$ rad./sec. initial amplitude of oscillation during the short period;

$$n = \frac{V\dot{\theta}}{g} + 1 = \frac{219(.08)}{32.2} + 1 = 1.5 \text{ g's}$$

MOD. NAV.: Computer equations:

Lift: $\dot{u} + .0297u - .0592\alpha + .1825\theta = 0$

Drag: $\dot{\alpha} + .3655u + 2.02\alpha - \dot{\theta} = 0$

Moment: $\ddot{\theta} + .730u + 5.32\alpha - .641\alpha + 1.038\dot{\alpha} + .0518\theta + 2.22\dot{\theta}$

$- 3.78\dot{\theta} - 15.75 K_s \delta_s = 0$

Damping and Period:

Phugoid	$T_{1/2} = 39.0$ sec.,	$P = 35.5$ sec.
Short Period	$T_{1/2} \doteq .5$ sec.,	$P \doteq 4.8$ sec.

Transient values: For .05 rad. δ_e (up elevator) step input, amplitudes of initial oscillations are as follows:

$u = -10$

$\alpha = +83^{\circ}$

$n = 6.8$ g's

For .05 rad. δ_e (up elevator) impulse

forcing function, initial oscillations:

$\delta_e = 12^{\circ}$ [Function of feed-backs]

$u = -.75$

$\alpha_{sp} = 16^{\circ}$

$\alpha_{phu} = 4^{\circ}$

$n = 3.2 - 4.0$ g's

COMPARISON OF TRANSFER FUNCTIONS

The denominator term common to all of the airplane transfer functions (not including auto-pilot dynamics) may be written as:

$$\Delta(S) = -h\tau^{4}(S-\lambda_1)(S-\lambda_2)(S-\lambda_3)(S-\lambda_4),$$ where

$\lambda_1, \lambda_2 \ldots\ldots \lambda_4$ are the roots of the characteristic equation (A4D-2 or MOD.NAV.). Numerator terms may be written as follows:

$$N_u = +C_{m_{\delta_e}}\delta_e\tau\frac{C_{D_\alpha}}{2}\left[S+\frac{C_{L_\alpha}C_L}{2\tau C_{D_\alpha}}\right]$$

$$N_\alpha = -C_{m_{\delta_e}}\delta_e\tau^2\left[S^2+\frac{C_D}{\tau}S+1/2\left(\frac{C_L}{\tau}\right)^2\right]$$

$$N_\theta = -C_{m_{\delta_e}}\delta_e\tau^2\left[S^2+\frac{1}{\tau}\left(C_D+\frac{C_{L_\alpha}}{2}\right)S+\frac{1}{2\tau^2}\left(C_DC_{L_\alpha}-C_LC_{D_\alpha}+C_L^2\right)\right]$$

Now examine a typical transfer function, say $\frac{u}{\delta_e}(S)$:

$$\frac{u}{\delta_e}(S) = \frac{C_{m_{\delta_e}}C_{D_\alpha}}{-2h\tau^3}\,\frac{\left[S+\frac{C_{L_\alpha}C_L}{2\tau C_{D_\alpha}}\right]}{\left[(S-\lambda_1)\ldots\ldots\ldots(S-\lambda_4)\right]}$$

Evaluation of this transfer function gives:

$$\text{MOD. NAV.:} \; = \frac{1.941\left[S + 2.99\right]}{\left[(S - \lambda_1)\ldots\ldots(S - \lambda_4)\right]}$$

$$\text{A4D-2 :} \; = \frac{.492\left[S + .465\right]}{\left[(S - \lambda_1)\ldots\ldots(S - \lambda_4)\right]}$$

Now examine $\frac{\alpha}{\delta_e}(S)$:

$$\frac{\alpha}{\delta_e}(S) = \frac{C_{m_{\delta_e}}}{h\tau^2}\frac{\left[S^2 + 2\left(\frac{C_D}{2\tau}\right)S + \left(\frac{C_L}{\sqrt{2}\tau}\right)^2\right]}{\left[(S - \lambda_1)\ldots\ldots(S - \lambda_4)\right]}$$

This may also be written in servo-mechanism notation as follows:

$$\frac{\alpha}{\delta_e}(S) = \frac{K\left[S^2 + 2\zeta\omega_n S + \omega_n^2\right]}{\left[(S - \lambda_1)\ldots\ldots(S - \lambda_4)\right]}\;,$$ where

K is the gain, ζ is the damping ratio, and ω_n is the natural frequency of this minimum phase term (or second order lead term).

Evaluation of the transfer function gives:

$$\text{MOD. NAV.:} \; = \frac{-15.75\left[S^2 + 2(.0576)(.258)S + (.258)^2\right]}{\left[(S - \lambda_1)\ldots\ldots\ldots\ldots\ldots\ldots(S - \lambda_4)\right]}$$

$$\text{A4D-2 :} \; = \frac{-2.41\left[S^2 + 2(.162)(.208)S + (.208)^2\right]}{\left[(S - \lambda_1)\ldots\ldots\ldots\ldots\ldots\ldots(S - \lambda_4)\right]}$$

And examine $\frac{\theta}{\delta_e}(S)$:

$$\frac{\theta}{\delta_e}(S) = \frac{C_{m_{\delta_e}}}{h\tau^2}\frac{\left[S^2 + \frac{1}{\tau}\left(C_{D_\alpha} + \frac{C_{L_\alpha}}{2}\right)S + \frac{1}{2\tau^2}\left(C_D C_{L_\alpha} - C_L C_{D_\alpha} + C_L^2\right)\right]}{\left[(S - \lambda_1)\ldots\ldots\ldots\ldots\ldots\ldots\ldots\ldots(S - \lambda_4)\right]}$$

$$\text{MOD. NAV.:} = \frac{-15.75\left[s^2 + 2(3.58)(.286)s + (.286)^2\right]}{\left[(s-\lambda_1)\ldots\ldots\ldots\ldots\ldots(s-\lambda_4)\right]}$$

$$\text{A4D-2 :} = \frac{-2.41\left[s^2 + 2(2.17)(.164)s + (.164)^2\right]}{\left[(s-\lambda_1)\ldots\ldots\ldots\ldots\ldots(s-\lambda_4)\right]}$$

ROOT LOCUS STUDY OF FEED-BACKS

In a study of the feed-back quantities used to simulate the A4D-2, the characteristic determinant for the Navion must first be examined. With angles in radians, and in real time, the determinant is:

$$\begin{array}{ccc}
\underline{u} & \underline{\alpha} & \underline{\theta} \\
(C_D + \sigma p) & 1/2(C_{D_\alpha} - C_L) & \frac{C_L}{2} \\
C_L & \left(\frac{C_{L_\alpha}}{2} + \sigma p\right) & -\sigma p \\
 & (C_{m_\alpha} + C_{m_{d\alpha}}\sigma p) & (C_{m_{d\theta}} - h\sigma p)\sigma p
\end{array}$$

With the addition of a u feed-back in the moment equation, the moment equation takes the following form:

$$K_3 C_{m_{\delta_e}} u + (C_{m_\alpha} + C_{m_{d\alpha}}\sigma p)\alpha + (C_{m_{d\theta}} - h\sigma p)\sigma p\theta = -C_{m_{\delta_e}}\delta_e$$

Then the characteristic equation takes the following form:

$$-h\sigma^4(\lambda-\lambda_1)(\lambda-\lambda_2)(\lambda-\lambda_3)(\lambda-\lambda_4)$$

$$-K_3 C_{m_{\delta_e}}\sigma\frac{C_{D_\alpha}}{2}\left[\lambda + \frac{C_L C_{L_\alpha}}{2C_{D_\alpha}\sigma}\right] = 0,$$

where $\lambda_1 \ldots\ldots \lambda_4$ are the roots of the characteristic equation. Such roots naturally are modified by the root which is part of the second term of the equation. The equation may be further simplified:

$$\frac{a(\lambda - \lambda_1)\ldots\ldots\ldots(\lambda - \lambda_4)}{\left(\lambda + \frac{C_L C_{L_\alpha}}{2 C_{D_\alpha} \tau}\right)} - K_3 = 0,$$

where $a = - h \tau^3 / C_{m_{\delta_e}} C_{D_\alpha}$, and is a positive number. Then:

$$\lambda \doteq \left. \frac{- C_L C_{L_\alpha}}{2 C_{D_\alpha} \tau} \right|_{NAVION} = \frac{-(.493)(5.45)}{2(.333)(1.35)} = -2.99$$

Also, the roots of the characteristic equation of the Navion are:

$$\lambda_{phu} = - .0106 \pm .194i$$

$$\lambda_{s.p.} = - 2.64 \pm 1.67i$$

where "phu" indicates phugoid, and "s.p." indicates short period.

Refer to the root locus diagram, Fig. B2. For K_3 positive, or down elevator for increasing u, examine the 0° condition: it may be seen that damping and frequency of the short period mode are somewhat increased (period and time to damp to one-half amplitude, P and $T_{1/2}$, are decreased), but the characteristics of the phugoid mode are altered appreciably. The phugoid oscillation rapidly becomes unstable, then becomes aperiodic and divergent.

In like manner, feeding back α, $\dot{\theta}$, and θ, singly and in order, results in the addition of the following terms to the original Navion characteristic equation:

$$\alpha : \quad + K_1 C_{m_{\delta_e}} \mu^2 \left[\lambda^2 + \frac{C_D}{\mu} \lambda + \frac{C_L^2}{2\mu^2} \right]$$

$$\lambda = - .0147 \pm .258i$$

$$a = - h\mu^2 / C_{m_{\delta_e}} \ ; \ 0^\circ \text{ condition.}$$

$$\dot{\theta} : \quad + K_2 C_{m_{\delta_e}} \mu^2 \lambda \left[\lambda^2 + \frac{1}{\mu}\left(C_D + \frac{C_{L_\alpha}}{2}\right)\lambda + \frac{C_D C_{L_\alpha}}{2\mu^2} - \frac{C_L}{2\mu^2}\left(C_{D_\alpha} - C_L\right) \right]$$

$$\lambda = 0, \ - 2.01, \ + .04$$

$$a = - h\mu^2 / C_{m_{\delta_e}} \ ; \ 0^\circ \text{condition}$$

$$\theta : \quad + K_4 C_{m_{\delta_e}} \mu^2 \left[\lambda^2 + \frac{1}{\mu}\left(C_D + \frac{C_{L_\alpha}}{2}\right)\lambda + \frac{C_D C_{L_\alpha}}{2\mu^2} - \frac{C_L}{2\mu^2}\left(C_{D_\alpha} - C_L\right) \right]$$

$$\lambda = - 2.01, \ + .04; \ 180^\circ \text{ condition}$$

For the results of the root locus studies, refer to Figs. B2 through 5. For a summary of results of Appendix B, refer to Tables I and II.

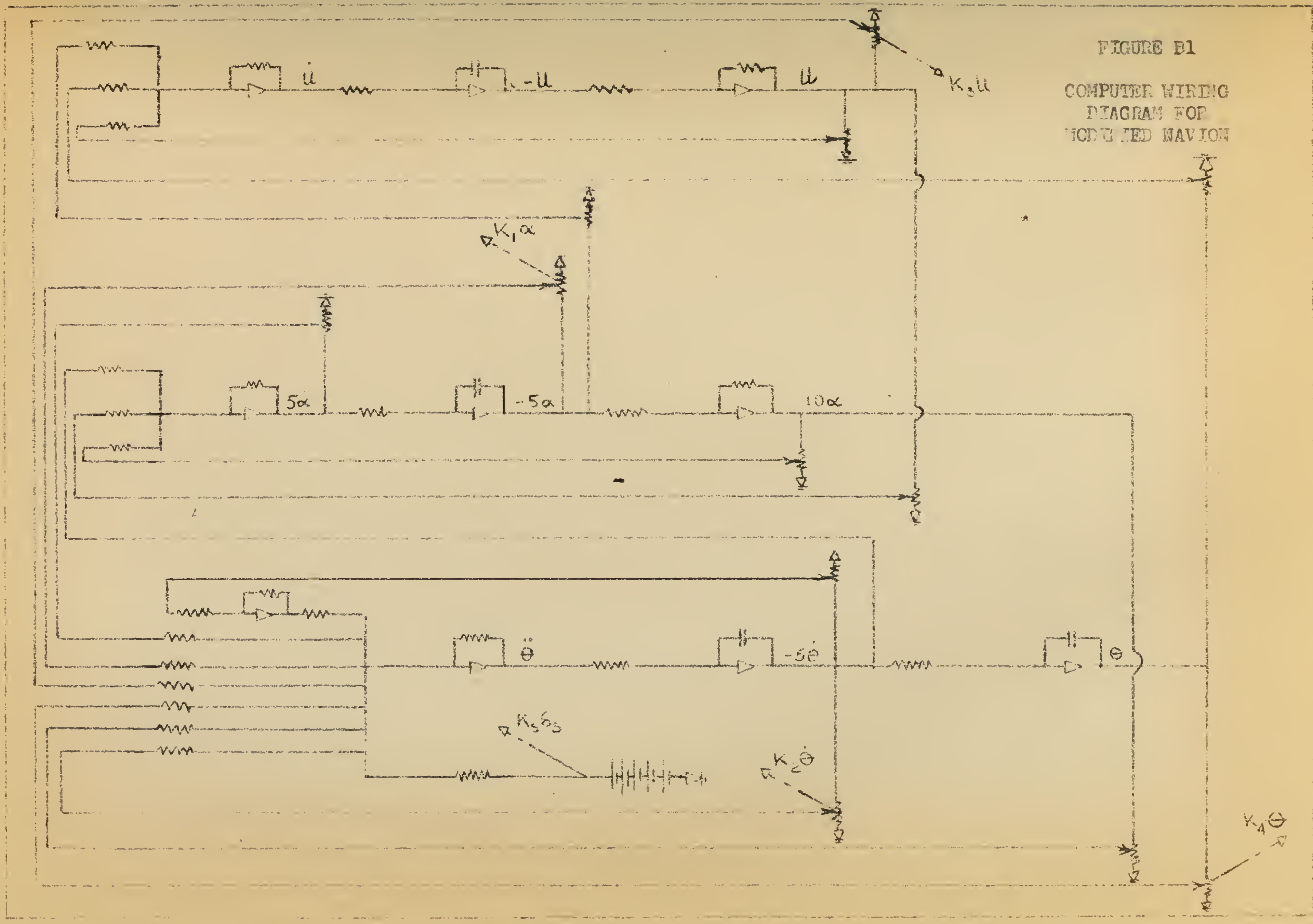

FIGURE B1

COMPUTER WIRING
DIAGRAM FOR
MODIFIED NAVION

FIGURE B1 concluded

Auxiliary Circuit for Elevator Deflection

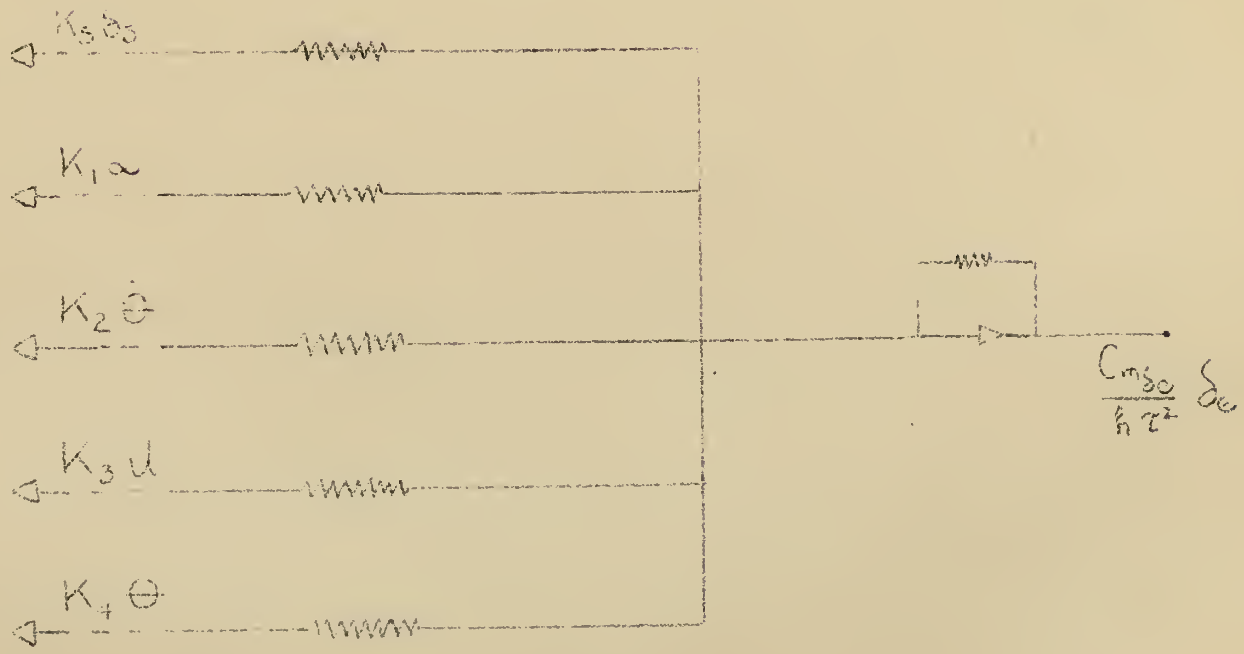

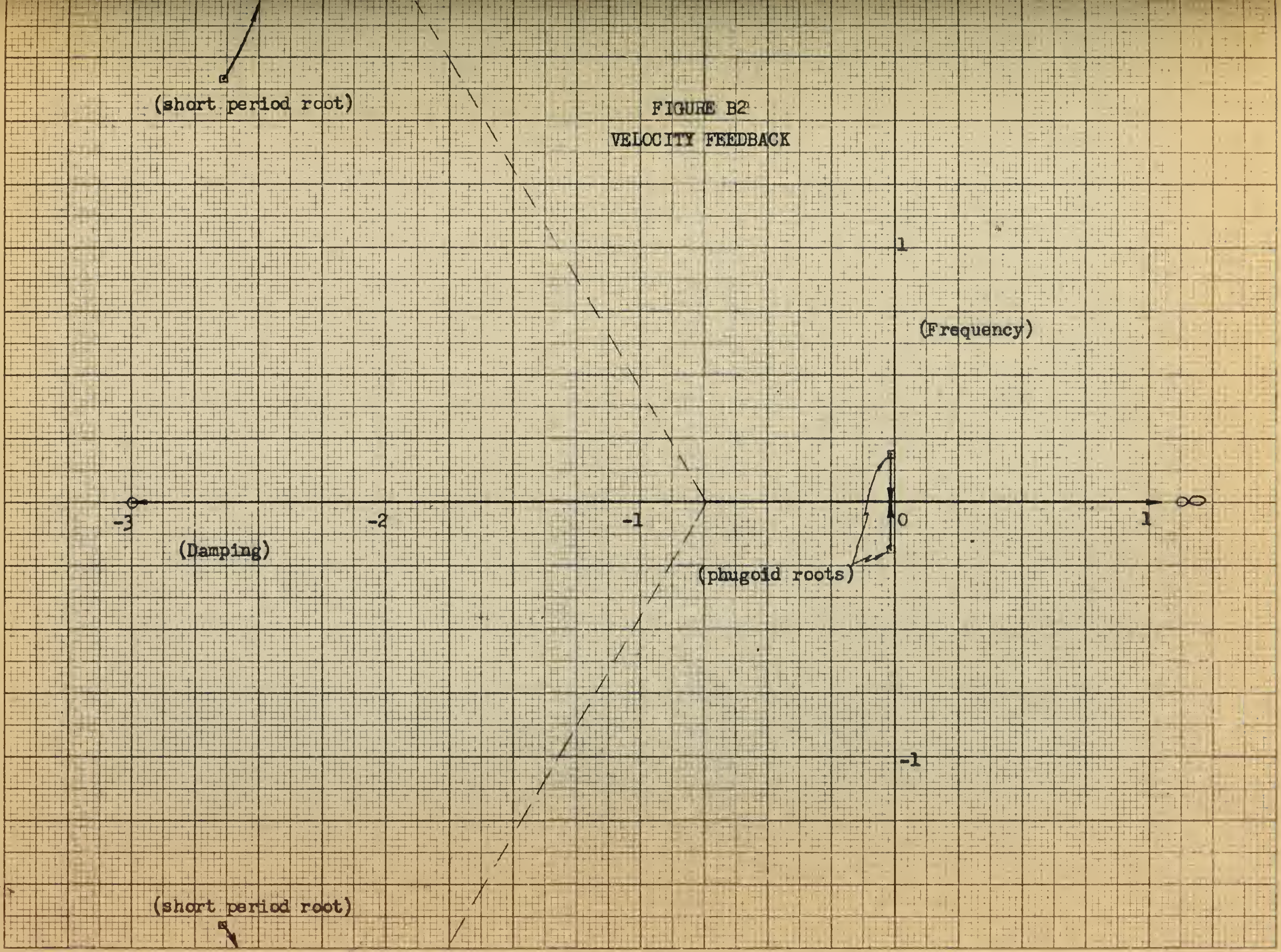

FIGURE B2

VELOCITY FEEDBACK

FIGURE B3

ANGLE OF ATTACK FEEDBACK

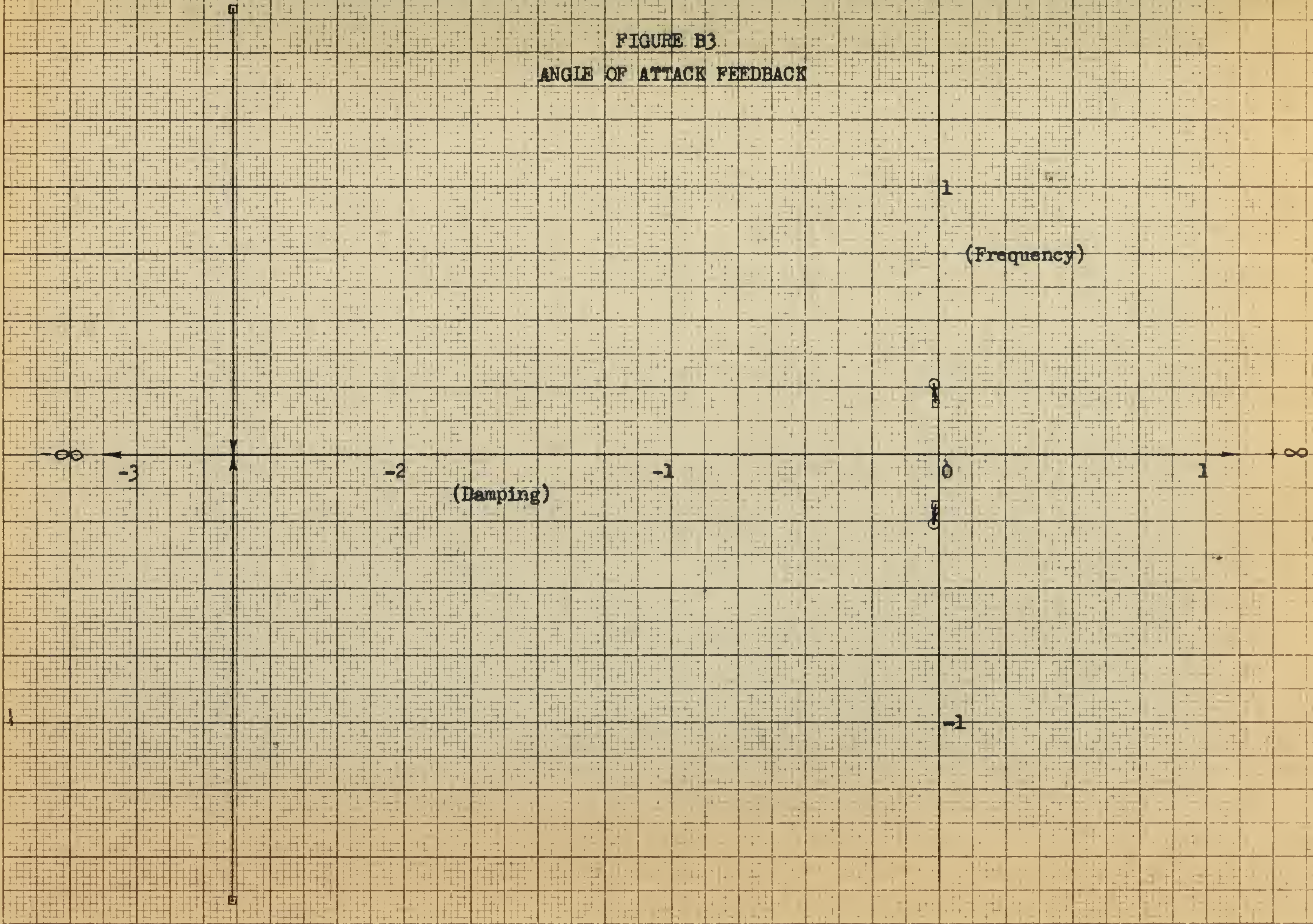

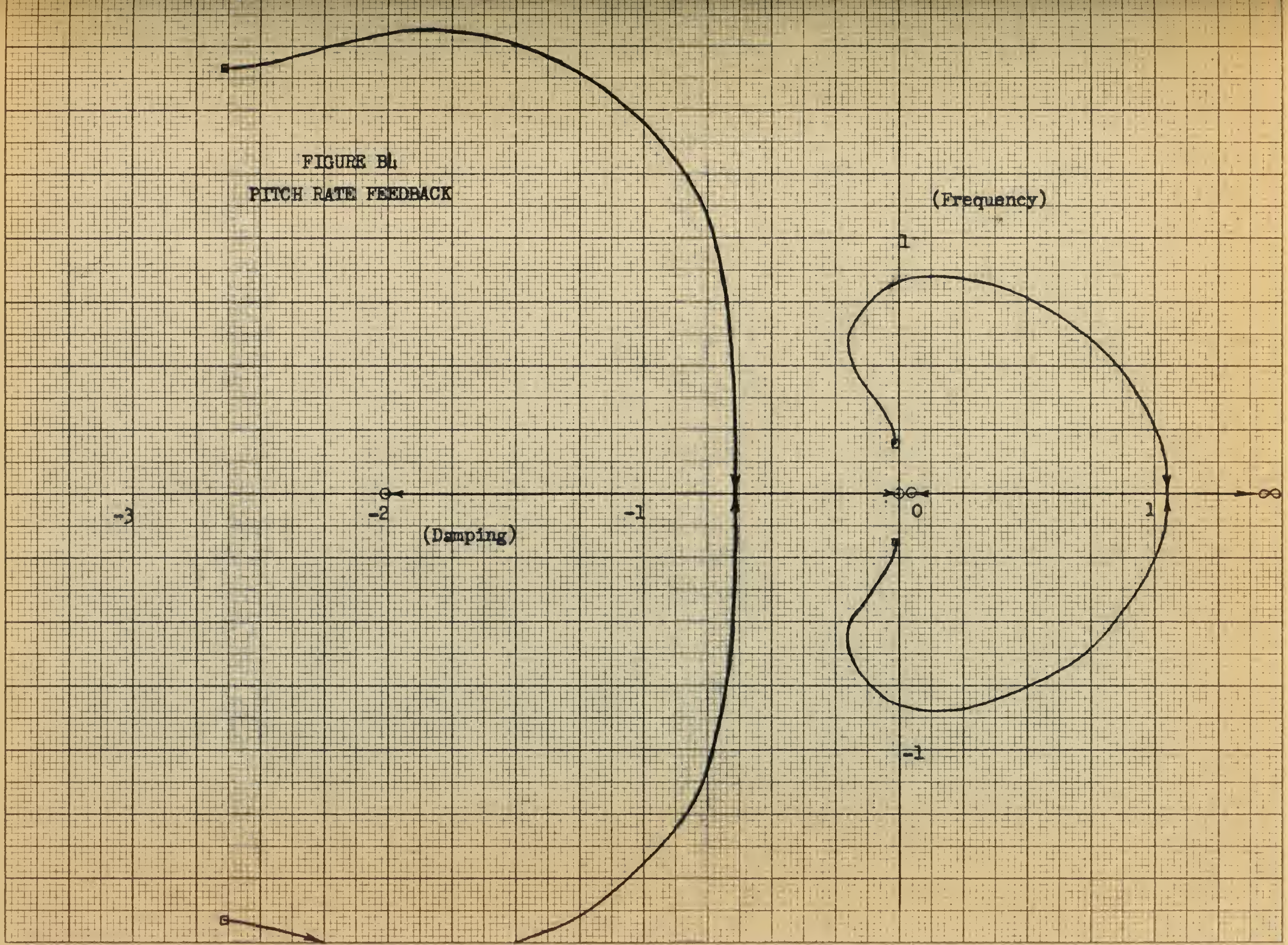

FIGURE B4

PITCH RATE FEEDBACK

FIGURE B5

PITCH ANGLE FEEDBACK

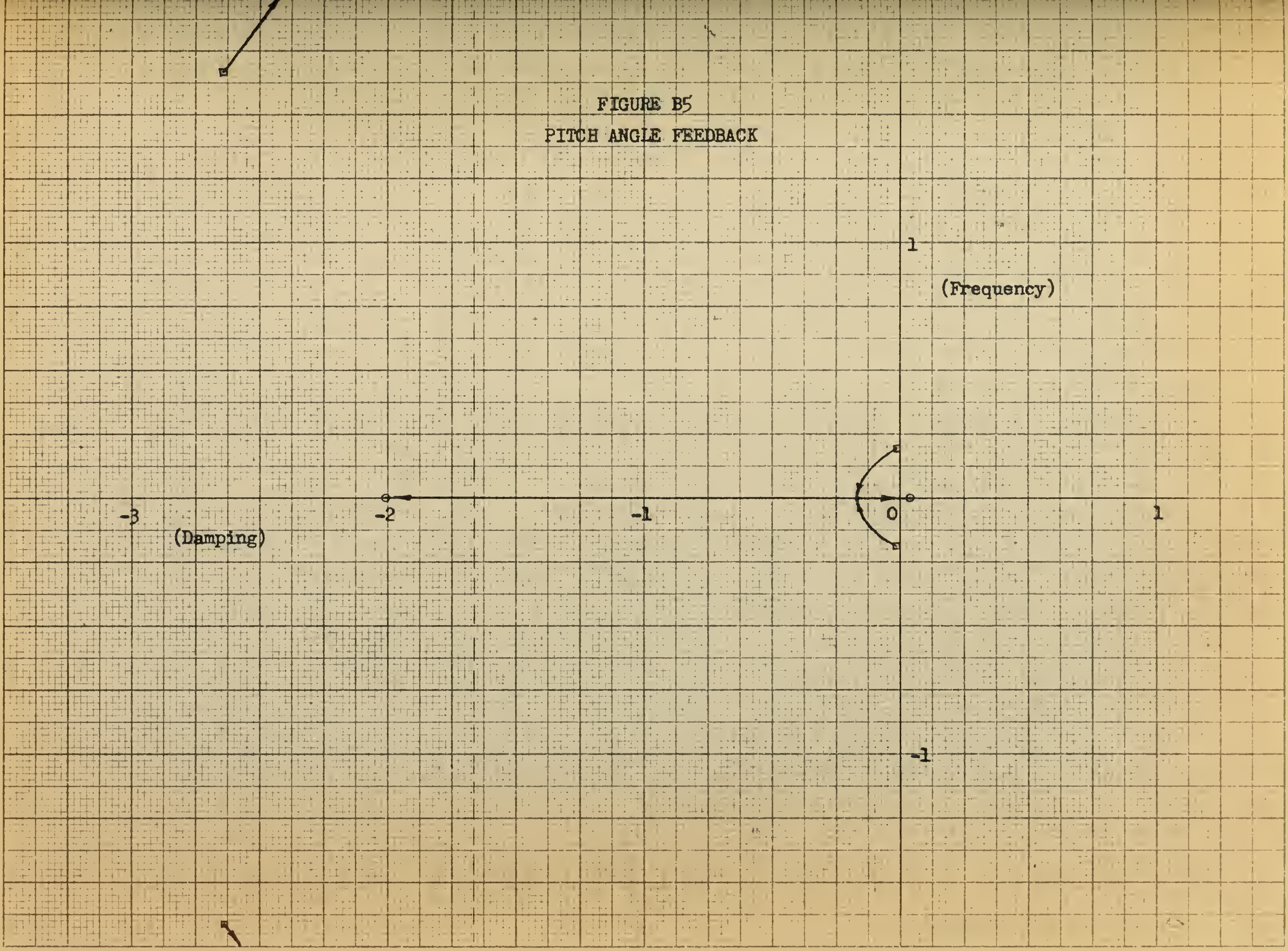

APPENDIX C

VARIABLE-STABILITY INSTALLATION

The selection of the Minneapolis-Honeywell, USAF TYPE E-12, Auto-pilot imposed some limitations on the force and speed of response available for control surface movement. Flight test results, presented in Figs. C1 and C2, showed that the force requirements of the vehicle for the variable-stability installation, Princeton University's North American Navion, (Fig. C3), were well within the 160 in. lb. shaft-torque output of the servo motors. The speed and frequency response characteristics were studied by another group working on the installation and are discussed in Ref. 9.

Blueprints of an auto-pilot installation designed for the Navion were obtained from Lear, Inc. From this basic design two brackets were made of 1/8", 24-ST, aluminum sheet and bolted to the partial bulkhead at the after end of the baggage compartment. Across these vertical brackets a 1/8", 24-ST, aluminum plate was bolted such that the plate lay in a plane approximately 90° to the ship's control cables. To support the servo motors a four-sided box, about eleven inches square, was fabricated of 1/8", 24-ST, aluminum sheet and 3/4" by 1/8", 17-ST, aluminum angle extrusions. To each of three sides of the box a servo was bolted, the bolts extending through aluminum angle stiffeners on the inner faces of the box sides. The remaining side of the box was bolted to the plate and bracket combination. Additional stiffening was supplied by 1/16", 24-ST, aluminum sheeting across the top and bottom of the box and two small 1/8", 24-ST, sheet metal fillets

bolted to the vertical brackets and the partial bulkhead as lateral supports. The entire servo mount was over-designed to preclude structural vibrations; the completed unit is shown in Fig. C4.

With the servos mounted vertically the capstans, or motor-driven pulleys, were nearly parallel with the ship's rudder and elevator cables. The bridle cable from the elevator servo, made of 3/32" aircraft control cable, was fastened to the capstan and fed directly aft about five feet to join the elevator cables at a small angle. The 1/8" rudder bridle cable was wrapped around the capstan and fed directly aft on the right side; a two in. fiber pulley was mounted on the under side of the sheet metal box to aline the bridle cable with the left rudder cable. The aileron bridle, of 1/8" cable, also was wrapped around its capstan, and the free ends of the bridle were fed forward through existing cable access holes in the bulkhead; a two in. fiber pulley was necessary for alinement on the right side. The 1/8" bridle cable was then mated to the 3/32" cross-control cable, the latter having been disconnected from the rudder cables. Standard aircraft cable thimbles and turnbuckles were used in all cable connections. The rudder and elevator bridles were attached to the ship's cables using sheet metal c-clamps. The bridle cable was united with the clamp by a 3/16" bolt passing through a thimble and the clamp; the clamp was tightened around the control cable with three more bolts. After completion of the bridle and cable matings, turnbuckles were adjusted for 25# tension in all bridle cables and 30# tension in the ship's cables. Servo clutch slip levels were adjusted to allow overpowering of the auto-pilot with reasonable control forces. The electrical servo stops were set to prevent

full deflection of any control surface in response to auto-pilot signals. A schematic diagram of the bridle-control cable arrangement is shown in Fig. 2.

The conventional yoke and rudder pedals were removed from the right side of the cockpit. Two spring-loaded rudder pedals were mounted on the floorboards; a small cable attached to the pedals was used to drive a 360° potentiometer. The electric stick, a spring-centered flight controller with adjustable fluid damping, was bolted to a pedestal for appropriate height. The flight controller had no provision for stick force inputs; it had a small break-out force that was not objectionable. In addition to the above, Fig. 5 shows the auto-pilot trim box as it was mounted adjacent to the flight controller.

Other modifications to the cockpit included the various auto-pilot and telemetry power switches mounted to the left of the instrument panel and the feed-back gain potentiometers grouped between the two front seats (see Fig. C6). The gain potentiometers are wire-wound potentiometers of approximately 5000 ohms each. With these feed-back controls eight aircraft responses (ϕ, $\dot{\phi}$, θ, $\dot{\theta}$, β , α and u) may be fed into the auto-pilot to vary the response, and hence the dynamic stability, of the aircraft. Control surface travel can be varied by either the stick and rudder pedal gain potentiometers or by the servo follow-up gain controls.

The major portion of the variable-stability installation was located in the baggage compartment just aft of the rear seat. The top shelf of a table was devoted to terminal strips that gave accessibility to the wiring of the system. These strips made it possible to monitor all the sensor

and excitation voltages; also, the sense of control deflection, for example down elevator for increasing u, could be changed at the terminal board merely by interchanging the transformer leads exciting the signal generator. The power to excite the primaries of the four multiple-wound transformers came from an inverter which converted the aircraft 28 volt d.c. supply to 115 volt, single phase, 400 cycle a.c.

The electronic portions of the auto-pilot were placed on a lower shelf along with two rate gyros and the pitch-roll attitude gyro; three more rate gyros were mounted on the floor of the baggage compartment (Fig. C7). Although only three rates of response were measured a separate gyro was required for each channel using the rate signal. The directional coupler feed-back loop and the control stick and co-ordinated turn capabilities of the auto-pilot were eliminated. An electronic safety device was adjusted to disengage the auto-pilot, by releasing the servo clutches allowing the capstans to rotate freely, if an error voltage of approximately three volts suddenly appeared as an input to any servo amplifier. A disengage switch on the control stick was wired also, along with another disengage switch, for the safety pilot, adjacent to the main power switch.

To record in-flight data an ASCOP pulse width frequency modulating telemeter station was used. The 15 channel filter conversion unit and the rotary sampling switch and transmitter unit were mounted in the baggage compartment (Fig. C4). The filter conversion unit allowed sampling of fourteen signals, reserving one filter for reference voltage. The rotary sampling switch operated at 20 cps and could sample 43 quantities plus two zero readings; hence a telemetry terminal strip was made to

parallel switch channels so that each of the 14 filter outputs could be sampled three times per cycle. Additional data on the internal components of the auto-pilot may be found in Ref. 9.

To accommodate the remaining attitude sensors two booms were mounted, one at each wing tip rib as shown in Figs. C8 and C9. The booms, constructed for previous testing, placed the sensing devices about four feet in front of the leading edge, ahead of the major pressure disturbances around the wing. Dynamic and static pressure lines extend from the pressure probe to a differential pressure transducer mounted inside the wing. Two Giannini yaw vanes were orientated 90° apart on the left probe to serve as sideslip and angle of attack vanes; vane mutual interference was considered beneath the resolution of the system. Since two position potentiometers were actuated by each vane only one angle sensor was required to supply signals to both the yaw and roll channels.

To complete the installation it was necessary to calibrate the entire system, that is to determine sensor signal voltages, for various gain potentiometer settings, throughout the operating ranges of the various attitude and rate sensors. Also it was necessary to determine control surface deflection for given input voltages. Then, to enable reading of the telemeter traces, ratios of a.c. sensor signal voltage to d.c. telemeter signal voltage had to be established for each of the quantities to be recorded. Results of the longitudinal channel calibrations are shown in Figs. C10 and C11.

TABLE C1

ELECTRICAL COMPONENTS

Servo Motor	
Manufacturer	Minneapolis-Honeywell
Model No.	MG7001A-21
Weight	7.25 lbs.
Power Input	28 volts a.c., 9amps. max.
Power Output	160 in.lb. shaft torque
Maximum Limit Switch Spacing	± 112° drum rotation
Potentiometer Active Angle	± 125° drum rotation
Flight Controller	
Manufacturer	Minneapolis-Honeywell
Model No.	CG1A-1 (Pistol-grip-actuated)
Available Deflection	± 30° laterally and longitudinally maximum
Flight Controller	
Manufacturer	Minneapolis-Honeywell
Model No.	WG182A-2 (Knob-actuated)
	Used only for trim
Servo Amplifier	
Manufacturer	Minneapolis-Honeywell
Model No.	RG7064A-1
	Three stage voltage amplifier
Sideslip Vane	
Manufacturer	Giannini
Model No.	2516
Potentiometer Resistance	1997 ohms
Feedback Gain Potentiometer	5000 ohms

TABLE C1 concluded

Rate Gyros	
Manufacturer	Minneapolis-Honeywell
Model No.	JG7005A-24
Power Input	115 volts, 400 cycle a.c.
Rotor Speed	20,000 rpm
Weight	1.75 lbs.
Maximum Turn Rate	Modified to approximately 30 deg. per sec.
Potentiometer Resistance	530 ohms
Vertical Gyro	
Manufacturer	Minneapolis-Honeywell
Model No.	JG7003A-11
Power Input	115 volts, 400 cycle a.c., 30 watts (max)
Rotor Speed	20,000 rpm
Weight	4.5 lbs.
Potentiometer Active Angle	52 deg. either side of center
Angle of Attack Vane	
Manufacturer	Giannini
Model No.	2516
Potentiometer Resistance	2020 ohms
Telemeter Transmitter Unit	
Manufacturer	ASCOP
Model	DT-4
Input Signals	0-5 volts d.c.
Information Channels	43 plus two for synchronization of ground station
Sampling Rate	20 cps
RF Power Output	4 watts
Frequency Range	215-235 MC
Primary Power Requirement	28 volts d.c.
Weight	19.6 lbs.

FIGURE C1

Control Forces and Deflections

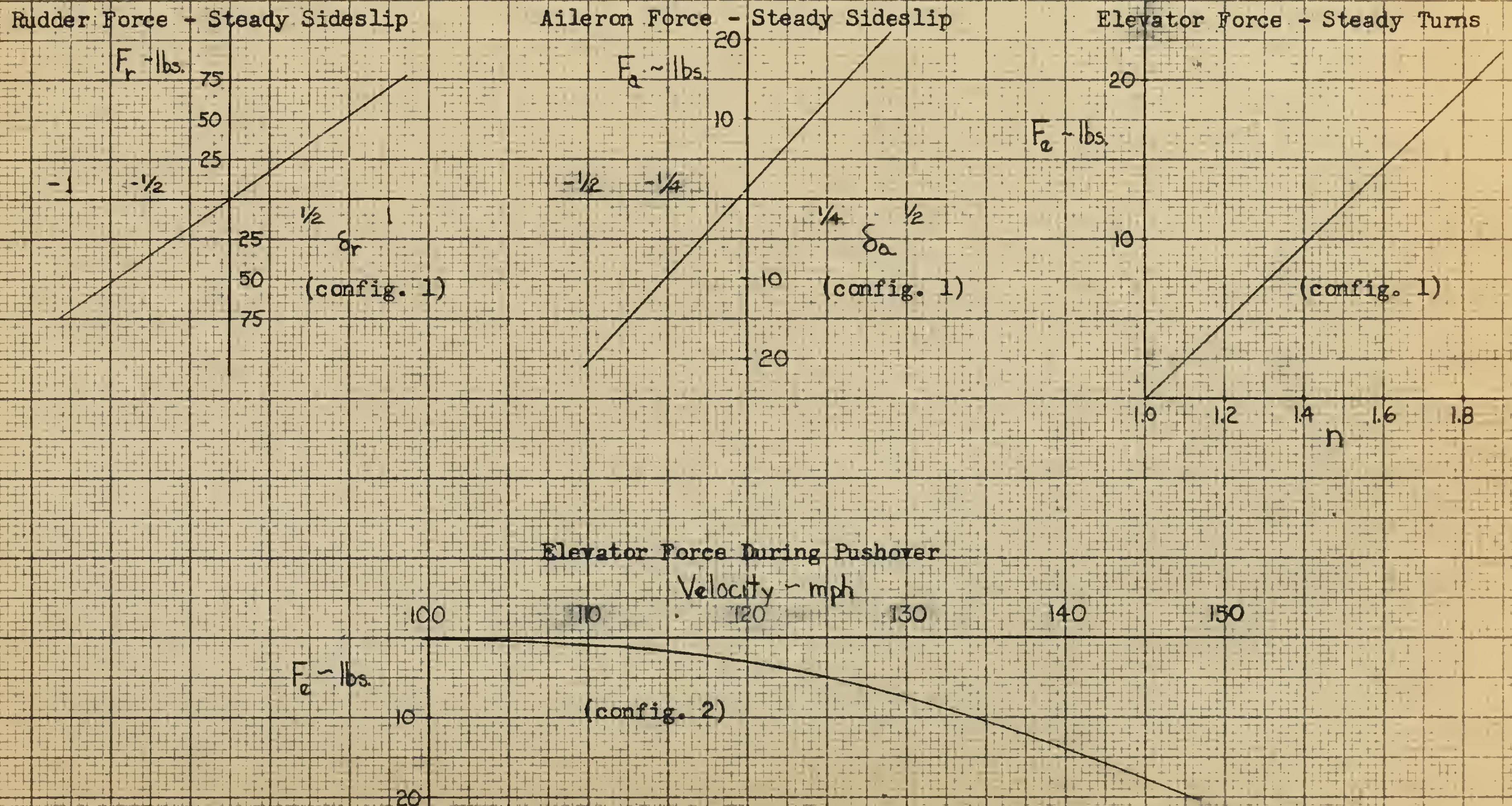

Configuration 1: clean, cowl flaps closed, mixture rich, trimmed at 122 mph, 22" map and 1900 rpm.
Configuration 2: clean, cowl flaps closed, mixture rich, trimmed at 100 mph, 19" map and 1750 rpm.

Pilot; Zink	Co-pilot; Wiltsie	Ryan Navion N5113K
Altitude - 1500'	c.g. = 26.5% MAC	Weight = 2600 lbs.

FIGURE C2

CABLE FORCES

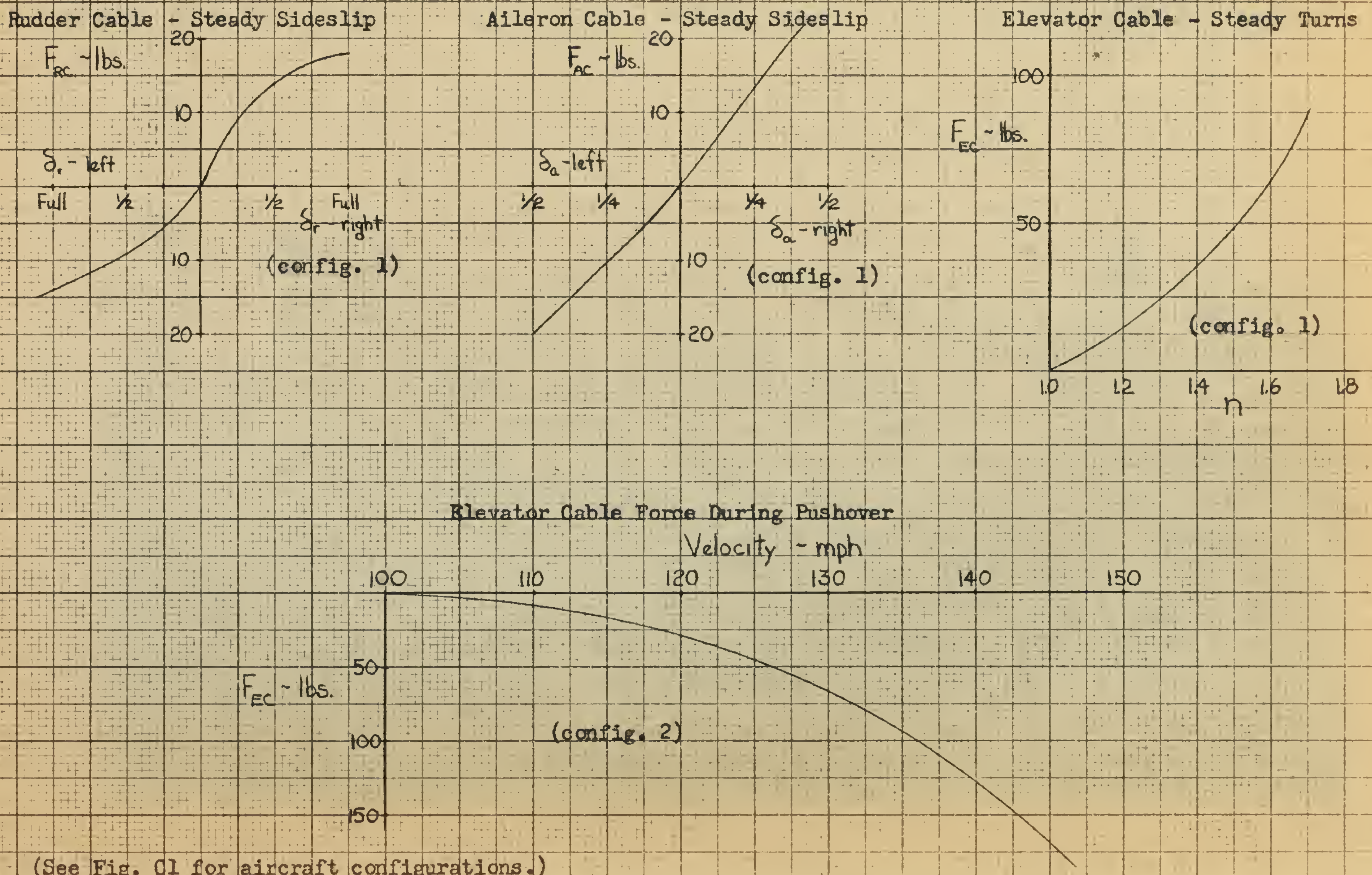

Rudder Cable - Steady Sideslip

Aileron Cable - Steady Sideslip

Elevator Cable - Steady Turns

Elevator Cable Force During Pushover

(See Fig. C1 for aircraft configurations.)

FIGURE C3

SIMULATOR AIRCRAFT

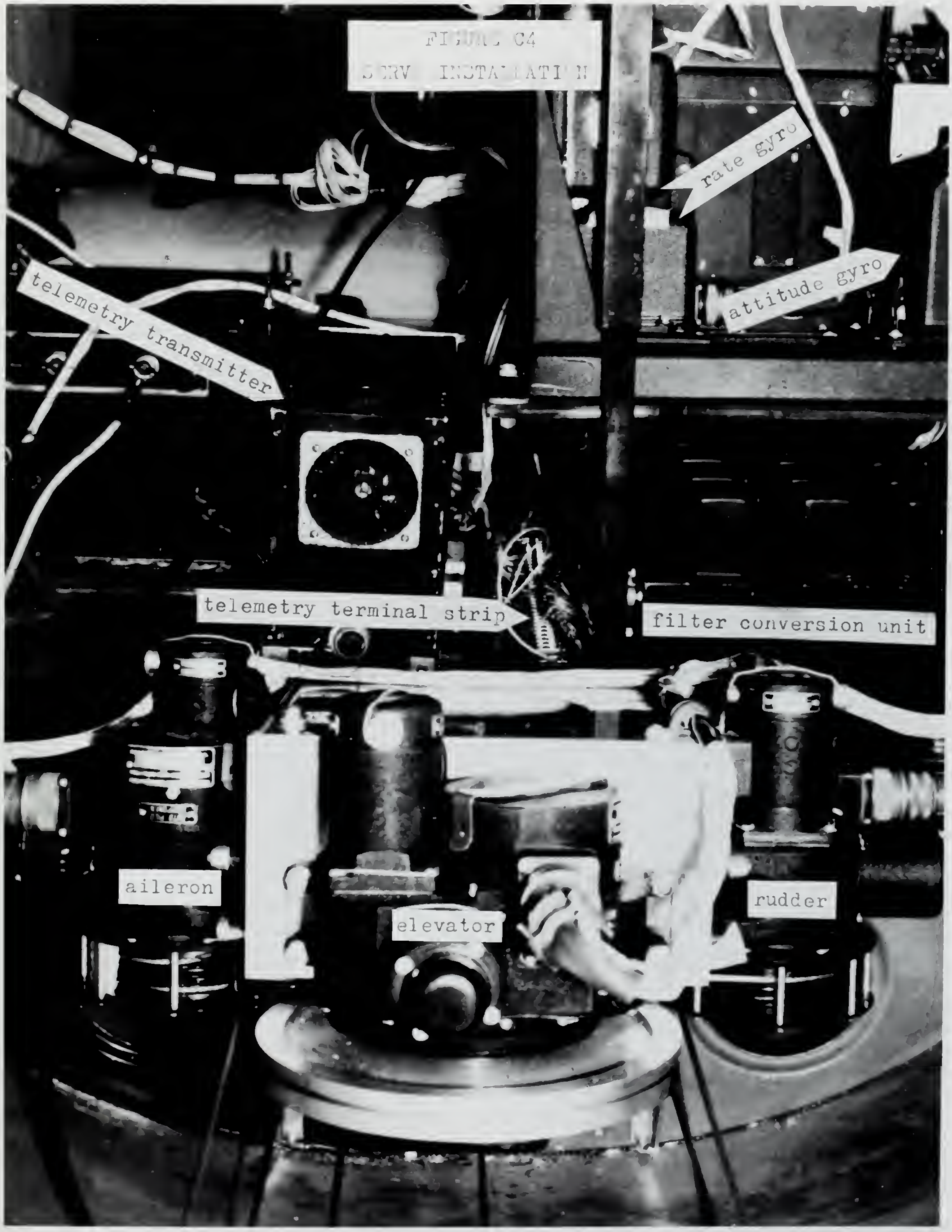
FIGURE C4
SERVO INSTALLATION

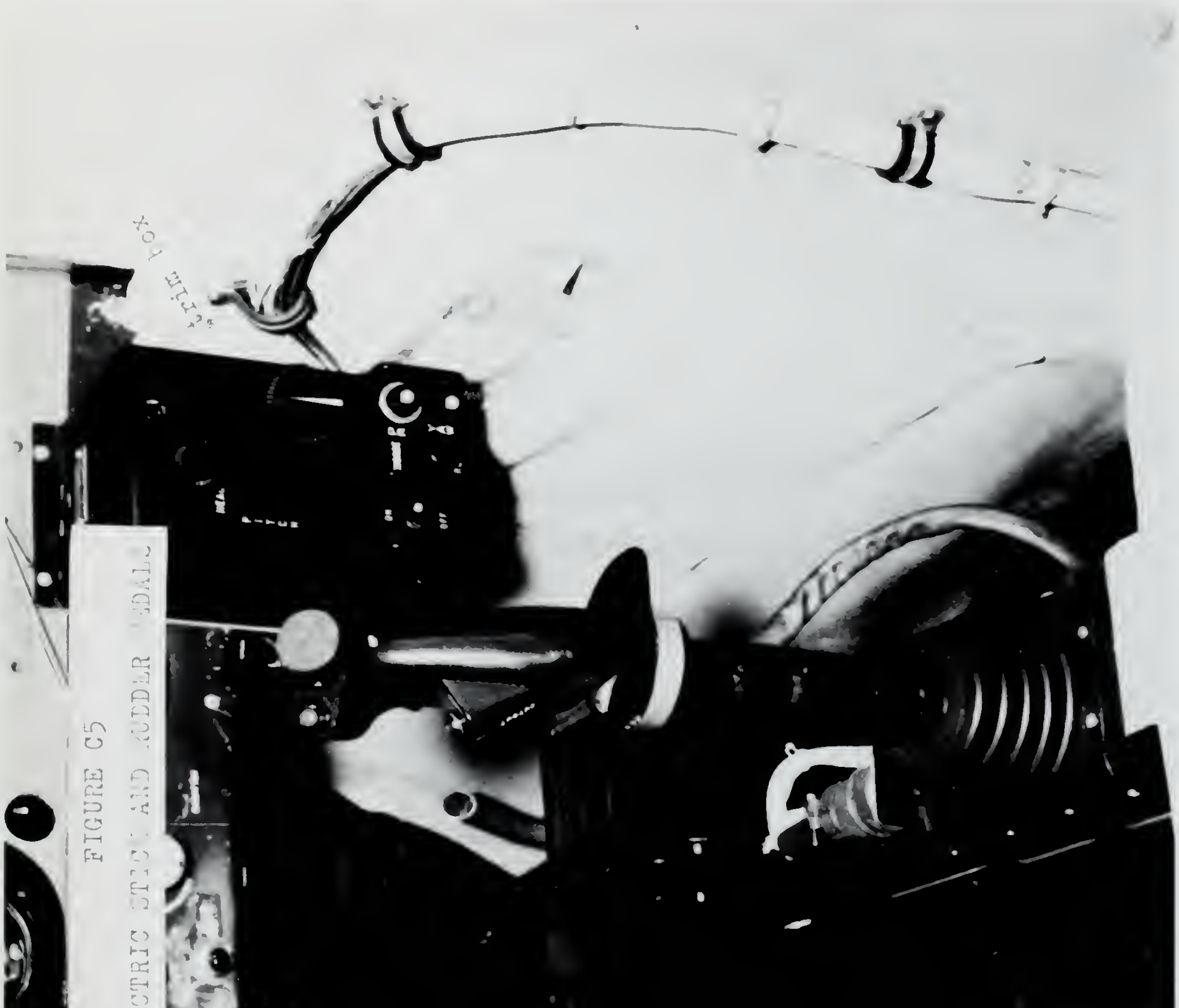

FIGURE C5

ELECTRIC STICK AND RUDDER PEDALS

FIGURE C6

FEED-BACK GAIN POTENTIOMETERS

FIGURE C7
AUTOPILOT EQUIPMENT SECTION

FIGURE C8

PRESSURE PROBE

FIGURE C9

ANGLE PROBE

FIGURE C10

SYSTEM CALIBRATIONS

(a) Elevator Deflection

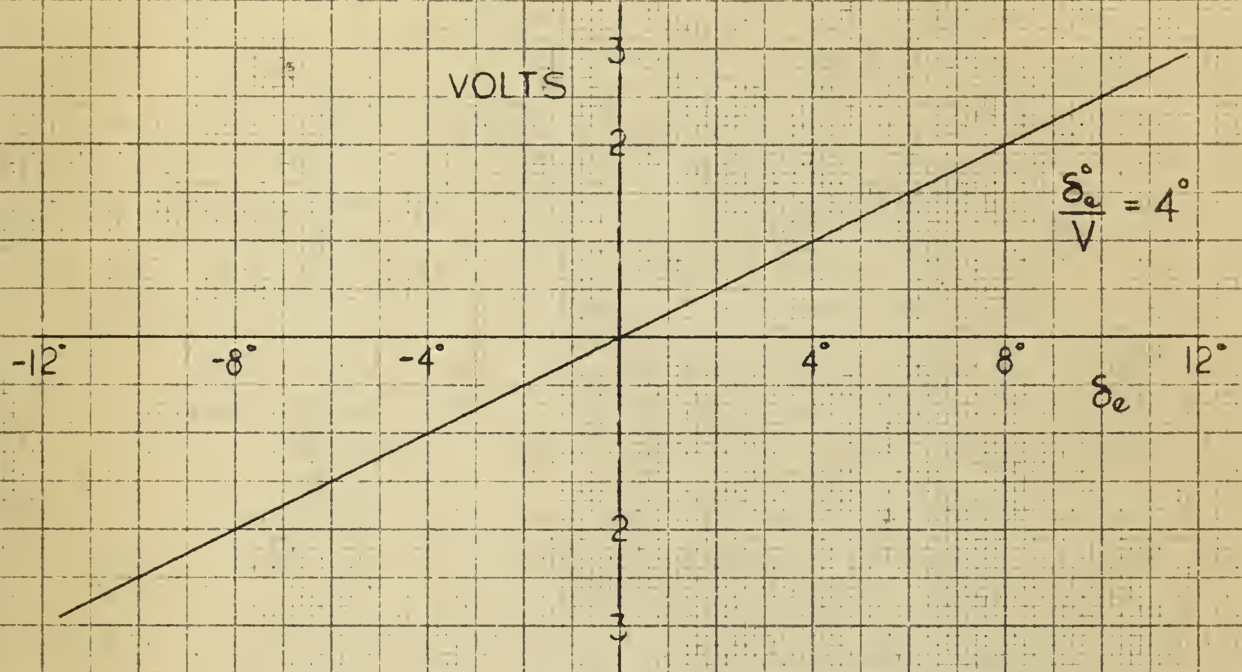

(b) Angle of Attack Vane

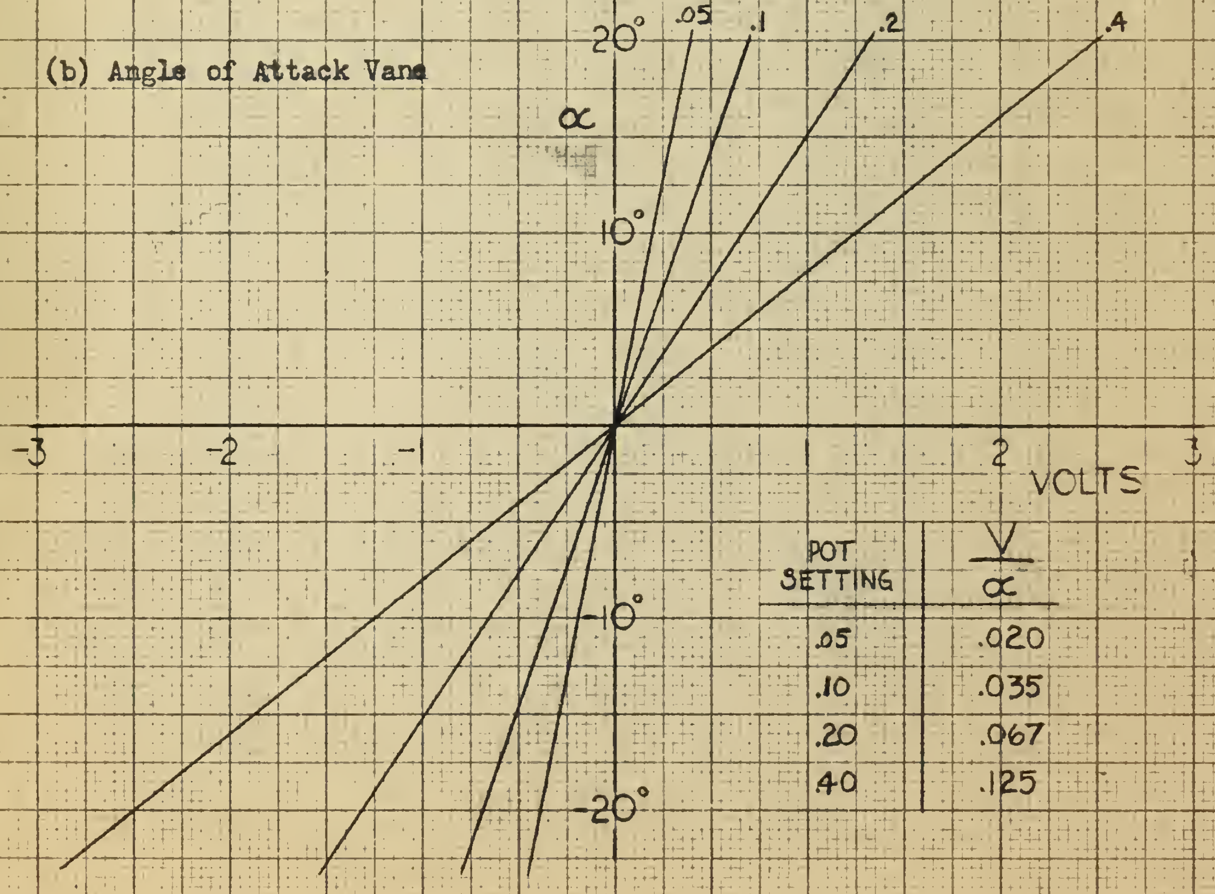

POT SETTING	$\frac{V}{\alpha}$
.05	.020
.10	.035
.20	.067
.40	.125

FIGURE C10 continued

(c) Pitch Rate Gyro

(d) Pitch Angle Gyro

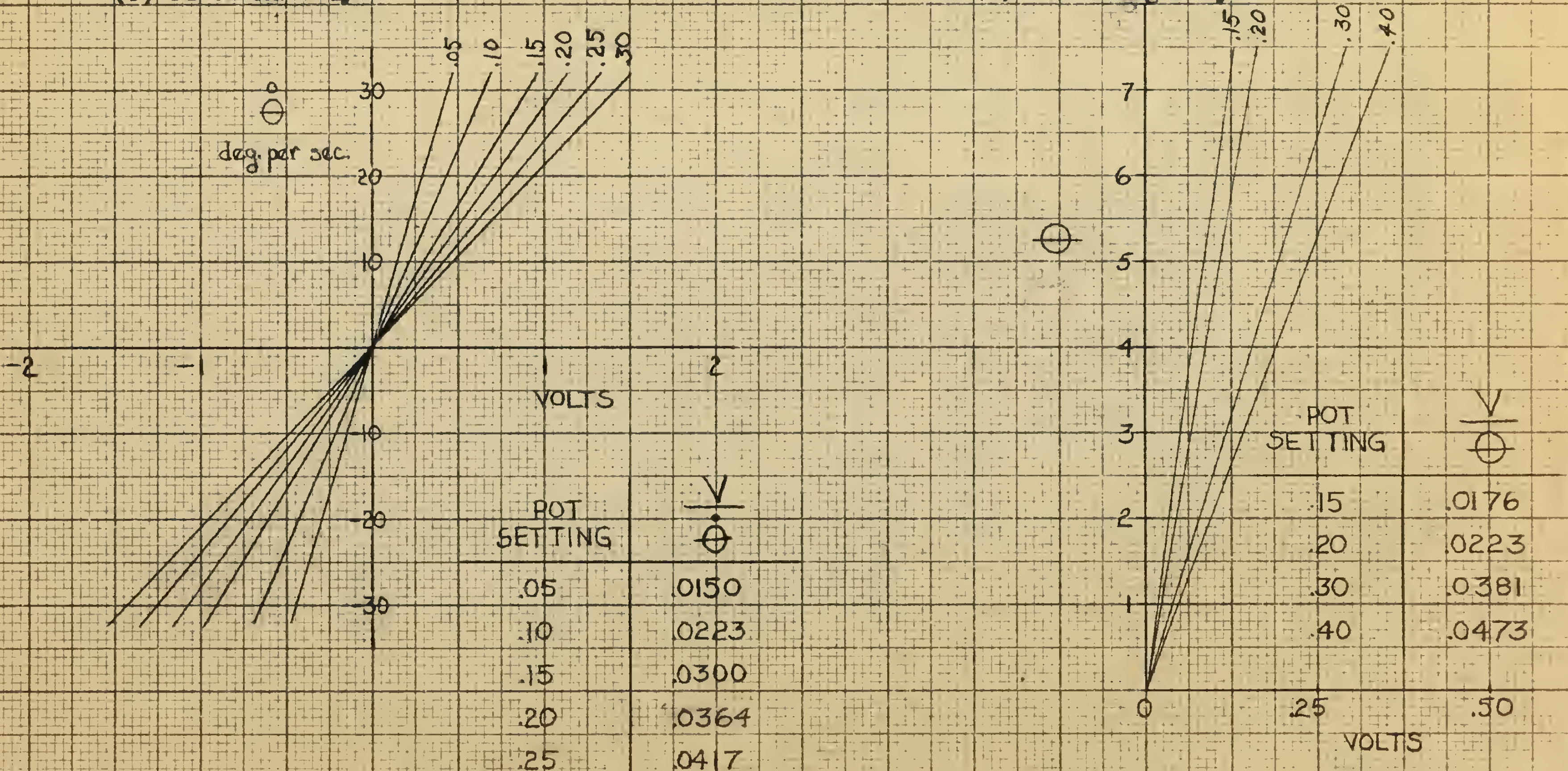

POT SETTING	$\frac{V}{\dot{\Theta}}$
.05	.0150
.10	.0223
.15	.0300
.20	.0364
.25	.0417
.30	.0474

POT SETTING	$\frac{V}{\Theta}$
.15	.0176
.20	.0223
.30	.0381
.40	.0473

FIGURE C10 concluded

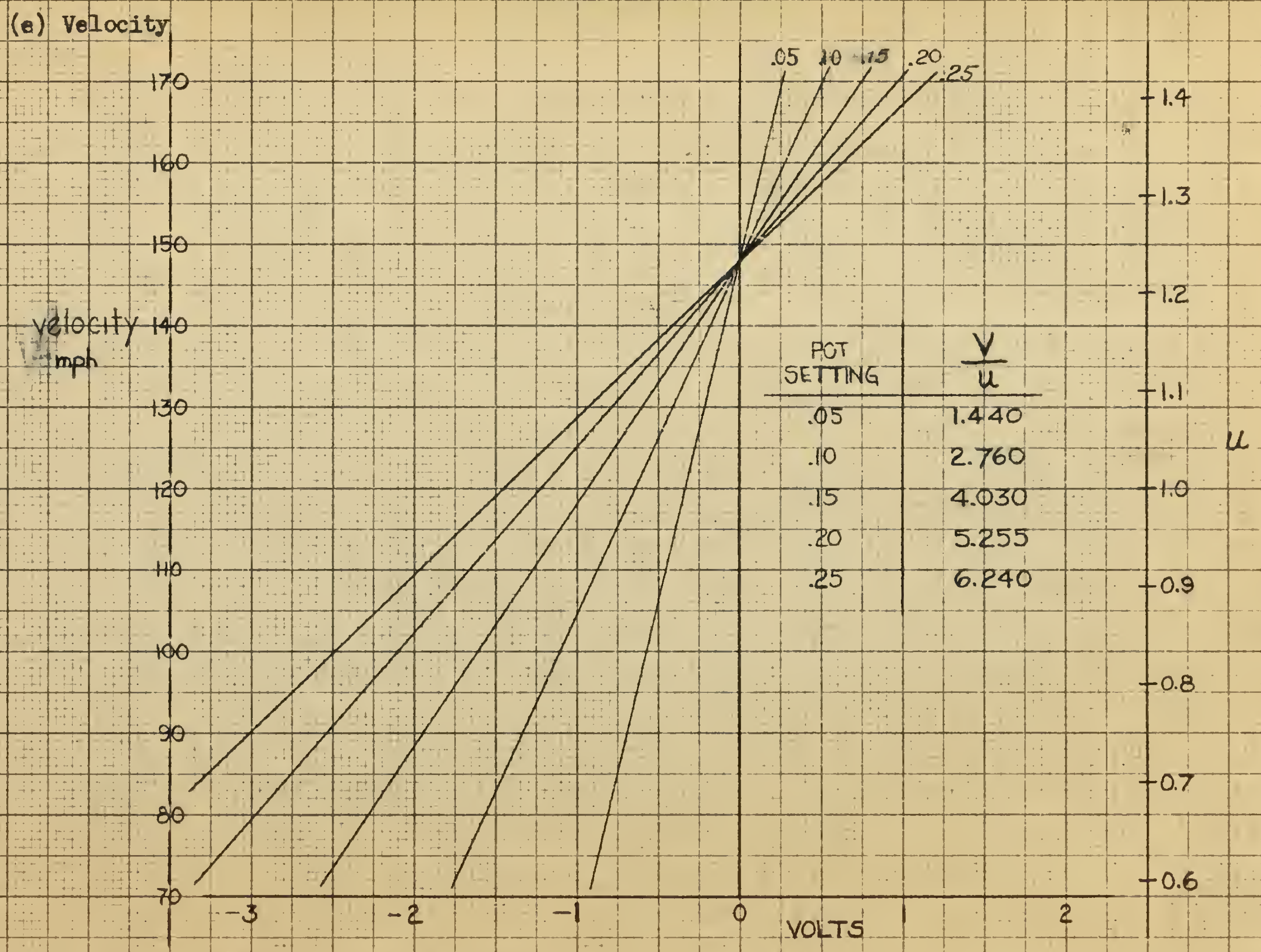

(e) Velocity

POT SETTING	$\frac{V}{u}$
.05	1.440
.10	2.760
.15	4.030
.20	5.255
.25	6.240

FIGURE C11

TELEMETRY VOLTAGE RATIOS